



# Spatial and temporal patterns of benthic nutrient cycling define the extensive role of internal loading in an agriculturally influenced oxbow lake

Rachel L. Nifong · Jason M. Taylor ·  
Stephen DeVilbiss

Received: 13 September 2021 / Accepted: 16 April 2022 / Published online: 9 May 2022

This is a U.S. government work and not under copyright protection in the U.S.; foreign copyright protection may apply 2022

**Abstract** Benthic habitats in shallow oxbow lakes may serve as permanent nitrogen (N) sinks by facilitating denitrification. Oxbow sediments may also accumulate nutrients through uptake, deposition and heterotrophic  $N_2$  fixation, and ultimately provide a significant internal source of N and phosphorus (P) through sediment release to the water column. To better understand nutrient source-sink dynamics in oxbow lakes, we explored seasonal and habitat specific patterns in sediment dissolved dinitrogen gas ( $N_2-N$ ) and nutrient flux within an oxbow in the Mississippi Alluvial Plain. Time series models indicate a higher probability of positive  $N_2-N$  fluxes in fall through spring, significant negative summer fluxes, and clear differences among habitats with net annual  $N_2-N$  fluxes, ranging from  $-2.34 \text{ g m}^{-2} \text{ Y}^{-1}$

in open water habitat to  $0.26 \text{ g m}^{-2} \text{ Y}^{-1}$  in shoreline areas. Integrated lake-wide  $N_2-N$  sediment flux estimates were negative indicating the significant role of net  $N_2$  fixation. More complex models explained similar amounts of variation ( $Adj. R^2 = 0.57$  vs.  $0.45$ ) and indicated that benthic  $N_2-N$  fluxes were associated with changes in temperature, dissolved inorganic N, sediment oxygen demand, and sediment carbon:N ratios. Ammonium and P flux from sediments were substantial across all habitats and internal N regeneration far outpaced removal from the system by sediment  $N_2-N$  flux. Results indicate that nutrient release from sediments generate internal nutrient loads proportional to external loading from the watershed. Our results highlight the significant potential for internal nutrient loading and benthic  $N_2$  fixation within sediments to regulate biogeochemical processes within understudied oxbow lake ecosystems.

Responsible Editor: Jack Brookshire.

**Supplementary Information** The online version contains supplementary material available at <https://doi.org/10.1007/s10533-022-00935-7>.

R. L. Nifong · J. M. Taylor · S. DeVilbiss  
Water Quality and Ecology Research Unit, Agricultural  
Research Service, United States Department  
of Agriculture, Oxford, MS 38655, USA

*Present Address:*

R. L. Nifong (✉)  
Southeast Watershed Research Laboratory, Agricultural  
Research Service, United States Department  
of Agriculture, Tifton, GA 31794, USA  
e-mail: Rachel.nifong@usda.gov

**Keywords** Nitrogen · Argon · MIMS · Agricultural watershed · Mississippi alluvial plain · LTAR

## Introduction

Oxbow lakes, formed by river meanders, are often embedded in heavily modified agricultural landscapes such as the Mississippi Alluvial Plain (MAP), where they can play a significant role in nutrient processing as they accumulate sediments and nutrients in runoff and from tens to thousands of square kilometers of

adjacent agricultural land (Schilling et al. 2019; Wren et al. 2019). Understanding their importance in nutrient cycles may be key to developing sound management strategies that promote agricultural production, wildlife habitat, and water quality improvements in intensively farmed areas. The MAP is an ideal region in which to evaluate their influence due to the overlapping intensity of agriculture and density of oxbow lakes (Locke et al. 2010).

Oxbow lake sediments may be an important regulator of benthic dinitrogen gas ( $N_2$ ) flux by serving as sites of different N cycling processes including denitrification, anammox (anaerobic ammonium oxidation), and  $N_2$  fixation. Denitrification is the transformation of reactive N in the form of nitrate ( $NO_3^-$ -N) or nitrite ( $NO_2^-$ -N), to  $N_2$  (Knowles 1982). Conditions within lake sediments may support denitrification or anammox, an alternate pathway that facilitates the direct conversion of fixed N as ammonium ( $NH_4^+$ -N) to  $N_2$  in aquatic ecosystems (Wenk et al. 2013). Together, denitrification and anammox both potentially contribute to the conversion of reactive and fixed N to  $N_2$  and overall N loss from benthic sediments to the atmosphere. In contrast,  $N_2$  fixation pulls  $N_2$  into lake ecosystems and converts it to organic  $NH_4^+$ -N. This process primarily occurs in cyanobacteria in lakes but can also occur in benthic sediments (Fulweiler et al. 2013) facilitated by heterotrophic, chemolithotrophic, chemoorganotrophic bacteria and archaea (Yao et al. 2018). The relative contributions of these three processes (denitrification and anammox vs.  $N_2$  fixation) dictate net positive or negative  $N_2$ -N fluxes with positive fluxes representing net sinks and negative fluxes representing net sources of bioavailable N to oxbow lake sediments.

The relative roles of denitrification, anammox, and  $N_2$  fixation in contributing to benthic  $N_2$ -N flux are affected by multiple factors including  $NO_3^-$ -N availability, oxygen, pH, temperature, and organic carbon (Knowles 1982; McCarthy et al. 2016). Spatiotemporal variability in these factors in agricultural watersheds makes elucidating patterns in  $N_2$  fluxes challenging because periods of significant flux may occur during short moments and within specific habitats. For example, temporal influences resulting in positive  $N_2$ -N fluxes including  $NO_3^-$ -N availability and dissolved organic (DOC) source, lability, and availability can range from short term pulses such as storm events (hours) to interannual variation (years) (Mengistu

et al. 2013) based on hydrologically linked seasonality of crop management practices (Royer et al. 2004; Royer and David 2005; Lizotte et al. 2017; Taylor et al. 2019). Moreover, sources of organic C are often spatially heterogeneous and can be transported across the landscape following preferential flow paths (Hill et al. 1999; Buttle and McDonald 2002; Lehmann et al. 2007). Heterogeneity across the landscape can enable proportionally small areas of land to contribute enough organic C to fuel nearly all of denitrification fluxes within receiving waterbodies (Duncan et al. 2013).

Spatial patterns in available organic C and its effect on  $O_2$  dynamics and N cycling processes are likely concentrated within oxbow lakes where the stage in the growing season, water column depth, and distance from shore mediate gradients of controlling factors. Nearshore littoral environment often supports submerged and emergent aquatic vegetation (Doi 2009), as well as flooded timber such as bald cypress (*Taxodium distichum*) and tupelo (spp) which contribute organic matter (OM) directly via litterfall or indirectly by trapping allochthonous materials in the nearshore zone of oxbow lakes (Lizotte et al. 2017). Furthermore, as light intensity decreases with depth, the influence of autochthonous contributions from aquatic shoreline vegetation and allochthonous contributions from nearby agricultural fields also decrease (Doi 2009). The influence of habitat zones on OM availability is particularly relevant for oxbow lakes within the MAP, which can be classified as discontinuous polymictic systems with weak short-term thermal stratification in late summer (Lizotte et al. 2017). Organic rich shoreline and cypress habitat zones can be quite narrow in oxbow lakes, requiring the deepest parts of the lake to potentially rely on autochthonous production to generate the OM and N necessary for denitrification during summer (Yoshii et al. 1999). Additionally, oxbow lakes and other small water bodies often represent discontinuities in size gradients embedded within drainage networks, potentially increasing residence time which may influence denitrification, anammox and  $N_2$  fixation by increasing processing efficiency (Harrison et al. 2009; Cheng and Basu 2017; Lizotte et al. 2017).

Despite the potential to provide ecosystem services by removing excess N through enhancing positive  $N_2$  fluxes from sediments, oxbow lakes have agricultural histories that can lead to storage of legacy nutrients

in lake sediments which, combined with inputs via  $N_2$  fixation, may maintain eutrophic conditions (Van Meter et al. 2016; Moriasi et al. 2020). Legacy nutrients increase the potential for oxbow lakes to provide ecosystem disservices through long-term release of N and phosphorus (P) from sediments, i.e., internal nutrient loading, creating a significant challenge to resource managers due to time lags between implementation of management practices to reduce eutrophication and actual lake ecosystem responses (Forsberg 1989; Meals et al. 2010). Ammonium, once released from sediments, can fuel prodigious, productive algal blooms (Paerl et al. 2015; Gardner et al. 2017). Legacy P fluxes from the sediment to the water column in the form of phosphate ( $PO_4^{-3}$ -P) can offset reductions in external P loads and increase available P to catalyze blooms during summer months, particularly in unstratified eutrophic or hypereutrophic shallow lakes (Welch and Cooke 2005; Burger et al. 2008; Sharpley et al. 2013; Paerl et al. 2020).

Identifying differences across habitats and seasons is important to elucidating key drivers of benthic nutrient cycling within low gradient oxbow lakes which will enable refinement of connections between agricultural production activities, hydrology, and ecosystem capacity to store and process N and P. These relationships are often difficult to discern, and extrapolation of habitat-specific nutrient fluxes to management activities can be challenging due to variability (Mosier et al. 1998; Seitzinger et al. 2006). Yet, as efforts to increase long-term sustainability of agriculture evolve, understanding when, under what specific habitat conditions, and at what rates N is removed or accumulated via  $N_2$ -N fluxes may influence management policies that reduce impacts of agricultural practices. Likewise, a more complete understanding of spatiotemporal patterns in sediment release of legacy N and P is needed to improve management of oxbow lakes in agricultural watersheds. In this study, trends in dissolved gas and nutrient fluxes were assessed by measuring rates and potential drivers between three separate habitat zones (shoreline, cypress, open water) and across seasons within an agriculturally influenced oxbow lake in the MAP. Dissolved nutrient and gas fluxes were measured during 14 separate flow-through laboratory incubations ( $n=201$ ) of sediment cores spanning 1 year. We hypothesized that high positive  $N_2$ -N flux rates would be concentrated in relatively small near shore zones

(shoreline, cypress) during periods of low productivity and high dissolved inorganic N (DIN) availability (winter/spring) and overall patterns would demonstrate that oxbow lakes serve as N sinks in the MAP due to their polymictic structure, ability to store and trap C, relatively long hydraulic residence time, and high N inputs. Alternatively, we hypothesized that release of N and P from lake sediments would result in net positive fluxes across all habitats, due to the potential for storage of legacy nutrients within oxbow lakes embedded within intensive agricultural watersheds, demonstrating that oxbow lakes are sources of both N and P within the MAP landscape. To test the broader hypotheses, we developed a model to predict temporal patterns in sediment  $N_2$ -N and dissolve inorganic nutrient fluxes from different habitats and estimate annual contributions to overall benthic nutrient cycling.

## Methods

### Field sampling

Beasley Lake is a shallow oxbow lake created as a meander cutoff of the Sunflower River sometime prior to 1940 within the MAP (USGS 2016). The lake has a relatively long residence time (87 day; Lizotte et al. 2017). It is polymictic with weak short-term stratification and eutrophic to hypereutrophic with chlorophyll *a* concentrations frequently exceeding  $25 \mu\text{g L}^{-1}$  during the summer (Locke et al. 2008). Vegetation around the lake is comprised of alligator weed [*Alternanthera philoxeroides* (Mart.) Griseb.], duckweed (*Lemna* sp.), and bald cypress trees (*Taxodium distichum*) which occur primarily along the shorelines and in the littoral zone; no submerged or floating macrophytes occur at depth (Lizotte et al. 2017). The 625 ha watershed is comprised of 150 ha of nonarable riparian wetland containing a mixture of bottomland hardwood and herbaceous wetland vegetation as well as 339 ha composed of arable land primarily planted to cotton (*Gossypium hirsutum* L.), soybeans [*Glycine max* (L.) Merr.], corn (*Zea mays* L.), and milo [*Sorghum bicolor* (L.) Moench]. During the time of this study, soy was the only crop planted. Beasley Lake watershed was first established as a research site in 1995 as part of the Mississippi Delta Management Systems Evaluation Area to evaluate Best

Management Practices (BMPs; Locke 2004). Later in 2003, the Lake was designated as one of 14 United States Department of Agriculture (USDA)–Agricultural Research Service (ARS) Conservation Effects Assessment Project (CEAP) watersheds for continued long-term assessment of BMPs and in 2014 was incorporated as a long-term agroecosystem research (LTAR) watershed research site (Lizotte et al. 2017).

We used flow-through laboratory incubations of intact sediment cores to evaluate net  $N_2$ -N fluxes using MIMS which provides direct and accurate measurements of  $N_2$ -N flux (Grantz et al. 2012). Due to the high frequency and spatial coverage of sediment coring events, we did not specifically measure any of the processes contributing to net  $N_2$ -N flux rates within our core incubations. Instead, we present net fluxes which we acknowledge ignores the balance of competing denitrification, anammox, and  $N_2$  fixation processes (McCarthy et al. 2016; Newell et al. 2016a). While some functional detail is lost, focusing on net fluxes still provides important information on source-sink dynamics of N related to  $N_2$  flux within our system. To measure net  $N_2$ -N fluxes in Beasley Lake sediments, sediment cores ( $n=201$ ) were collected on a biweekly to monthly basis from April 2017 through March 2018 at 5 transects: Transect 1 ( $33^\circ 24' 11.72''$  N,  $90^\circ 40' 13.47''$  W), Transect 1B ( $33^\circ 24' 3.66''$  N,  $90^\circ 40' 21.75''$  W), Transect 2 ( $33^\circ 23' 54.94''$  N,  $90^\circ 40' 33.73''$  W), Transect 2B ( $33^\circ 23' 48.98''$  N,  $90^\circ 40' 49.73''$  W), Transect 3 ( $33^\circ 23' 48.6''$  N,  $90^\circ 41' 1.2''$  W). Three cores were collected per transect, one for each of the three habitat types within the lake (shoreline, average  $0.6 \pm 0.03$  m ( $\mu \pm SE$ ) in depth; cypress, average  $1.2 \pm 0.08$  m in depth; and open water, average  $2.4 \pm 0.13$  m in depth). Intact benthic sediment cores were collected from the lake bottom along the transect using a manual corer consisting of a pvc pipe, a ball valve, and an attachment for holding acrylic coring tubes (surface area =  $40.6 \text{ cm}^2$ , height = 30–45 cm). The coring set up is designed to extract cores from shallow lakes while maintaining an undisturbed sediment water interface. Each intact core had approximately 12.3 cm of overlying water (500 ml volume). Sediment depths were approximately 18 cm for shoreline and cypress habitats and 33 cm for open water habitats. Open water habitats required deeper coring depths to obtain intact sediment cores. Previous studies have demonstrated that the bulk of sediment nutrient processing

occurs in shallow sediments (less than 5 cm) due to shallow diffusive boundary layers in littoral sediments (Lorke et al. 2003; Inwood et al. 2007) so effects of sediment coring depth on results should be minimal (though see Stelzer et al. 2011). Lake water (40 L) from each habitat type (shoreline, cypress, and open water) was collected and filtered using a canister filter ( $1\mu\text{m}$ ) into carboys. We used filtered water for incubations to attribute nutrient and dissolved gas fluxes to benthic processes by excluding microbial activity in the overlying water column and inflow water storage containers as much as possible (Miller-Way and Twilley 1996; Fulweiler et al. 2007; Larson et al. 2020; Li et al. 2021). Cores were capped on both ends and then transported along with carboys on ice to the USDA-ARS National Sedimentation Laboratory (NSL) in Oxford, Mississippi. Additionally, biweekly lake water quality samples (1 L removed 5 cm from the water surface) were collected at Transect 1, 2, and 3 (sensu Lizotte et al. 2017). Water quality samples were immediately chilled on wet ice ( $4^\circ\text{C}$ ) and transported to the USDA-ARS NSL, Oxford, Mississippi, for processing and analyses using standard methods (APHA 2005).

#### Laboratory incubations

In the laboratory, upper core caps were removed, and the cores were resealed with custom laser cut clear acrylic tops (Ridout Plastics, San Diego, California) attached with rubber 7.62 cm pvc pipe couplers (Pipeconx, Evansville, Indiana) for an airtight fit (Nifong et al. 2019). The tops were made with ports to connect Teflon™ tubing for inflow (American Wire Gauge (AWG) 20, 0.86 mm) and outflow (AWG 14, 1.63 mm) paths. Inflow tubing extended into the core just above the sediment–water interface while outflow tubing was flush with the core top on the interior of the core. During each sampling event, one control core (a 12.3 cm core lacking sediment,  $n=3$ ) was set up for each habitat type to account for potential physical effects related to a reaction with the core chamber materials.

Cores were incubated within a temperature-controlled environmental room (Model # MRW77810-CR; NOR-LAKE Scientific, Hudson, Wisconsin) set to average lake water temperature during sampling to reflect field conditions at core collection (Online Resource 1). Incubations were conducted in the dark

to prevent photosynthesis and oxygen bubble production, which can confound dissolved  $N_2$  gas measurements in closed-core systems (Kana et al. 1994; Gardner et al. 2006). Diurnal light–dark cycles can affect benthic processes; however, in Beasley Lake, shallow shoreline sites represent the only habitat where some light may reach sediments due to significant turbidity. Light penetration to the sediments is only likely to occur as secchi depths increase in late summer; yet during this time shoreline habitats are shaded by heavy canopy cover and phytoplankton are more concentrated reducing secchi depth 15 cm for every 1 m of decreased depth in agricultural lakes in the region (Henderson et al. 2021). Performing incubations in the dark should have minimal influence on interpretation of our results. Incubation water was equilibrated with the atmosphere using aeration stones and was pumped into cores at an average rate of  $1.4 \text{ mL min}^{-1}$  using a set of MV peristaltic pumps (Model # 7332-00; ISMATEC, Wertheim, Germany) for a residence time of just under 6 h.

Cores were allowed to flow continuously prior to sampling triplicate influent samples from each carboy and triplicate effluent samples from each core for dissolved gases and nutrients during three separate sampling times (24 h, 36 h, and 42 h post set up) over a three-day incubation period. For gas sampling, we filled 12 mL Exetainer® vials (Labco Limited, Lampeter, Wales) with core effluent water and allowed them to overflow three times prior to preservation with  $ZnCl_2$  (50% w:v). Vials were then sealed with caps with a chlorobutyl rubber septum. Dissolved gas samples were stored upside down in refrigerated, water-filled containers to prevent additional gas exchange until analysis. Filtered ( $0.45 \mu\text{m}$ ) influent and effluent samples were also collected to determine dissolved  $NO_3^-$ -N,  $NH_4^+$ -N, and  $PO_4^{3-}$ -P concentrations. All dissolved nutrient samples were frozen after collection until analysis (see below).

#### Water sample analysis

We sampled for water quality every 2 weeks for a total of 25 sampling events. Samples were characterized for dissolved and total nutrients, suspended sediments, as well as total suspended solids (TSS), alkalinity, hardness, turbidity, and chlorophyll *a*. Cadmium reduction and molybdate methods, following a micro-Kjeldahl block digestion, were used

to analyze total Kjeldahl N (TKN) and total P (TP). Dissolved  $NH_4^+$ -N,  $NO_3^-$ -N, and  $PO_4^{3-}$ -P concentrations for surface water grab samples and sediment core incubation samples were determined after filtration ( $0.45 \mu\text{m}$ ) using the phenolate, Cd reduction, and molybdate methods, respectively. All nutrient analyses were run on a Lachat QuickChem 8500 Series auto analyzer (Lachat Instruments, Loveland, Colorado). DOC of filtered samples ( $0.45 \mu\text{m}$ ) was also measured using an Apollo 9000 Combustion TOC analyzer (Teledyne Tekmar, Mason, Ohio). Additional analytes, including suspended solids, were measured according to standard methods (APHA 2005).

#### MIMS analysis

Dissolved gas samples from cores and microcosms were analyzed for  $N_2$  to argon ratios ( $N_2$ :Ar) and  $O_2$  to argon ratios ( $O_2$ :Ar) using a Membrane Inlet Mass Spectrometer (MIMS) equipped with a Pfeiffer PrismaPlus QME 220 mass spectrometer (Pfeiffer, Asslar, Germany) and a Bay Instruments S-25-75D membrane inlet (Bay Instruments, Easton, Maryland) (Kana et al. 1994). A solubility standard of purified water ( $18 \text{ M}\Omega$  resistance; E-Pure, Barnstead International) was equilibrated with the atmosphere using a circulating water bath set to the incubation temperature (VWR International) and by continuously stirring at 300 rpm (Caframo Limited) prior to analysis. The MIMS method assumes 100% Ar saturation, which varies due to temperature and salinity, but not due to biological production or consumption. Thus, biological effects on dissolved  $N_2$  in samples can be separated from physical effects using the Ar signal. Sample  $N_2$ :Ar and  $O_2$ :Ar ratios for each sample were converted to  $N_2$ -N and  $O_2$ -O concentrations based on the following equation (Grantz et al. 2012; Taylor et al. 2015):

$$[DG]_{\text{sample}} = \left( \frac{DG}{Ar_{\text{sample}}} \times [Ar]_{\text{expected}} \right) \left( \frac{[DG]/[Ar]_{\text{expected}}}{DG/Ar_{\text{standard}}} \right),$$

sample represents dissolved gas of the sample,  $DG/Ar_{\text{sample}}$  is the measured dissolved gas sample signal and  $DG/Ar_{\text{standard}}$  is the measured dissolved gas signal for well mixed, deionized water open to the atmosphere at the same temperature as the sample. The terms  $[Ar]_{\text{expected}}$  and  $[DG]/[Ar]_{\text{expected}}$  are the

theoretical saturated concentration and ratio, respectively, calculated for each in situ sample temperature using gas solubility tables (Weiss 1970).

Areal gas flux rates ( $DG_{flux}$ ,  $\text{mg m}^{-2} \text{h}^{-1}$ ) for each core were calculated as

$$DG_{flux} = \frac{([DG]_{out} - [DG]_{in})Q_{core}}{A} - \frac{([DG]_{control} - [DG]_{in})Q_{control}}{A} \quad (2)$$

$[DG]_{out}$ ,  $[DG]_{in}$ , and  $[DG]_{control}$  are the core chamber effluent, influent, and control chamber effluent dissolved gas concentrations ( $\text{N}_2\text{-N}$ ,  $\text{O}_2$ ) (in  $\text{mg L}^{-1}$ ), respectively;  $Q_{core}$  and  $Q_{control}$  are the measured flow rates through the core and control chambers (in  $\text{L h}^{-1}$ ); and  $A$  is the core surface area (in  $\text{m}^2$ ). The equation yields an aerial  $\text{N}_2\text{-N}$  flux and sediment oxygen demand (SOD) as  $\text{O}_2$  consumption for each independent intact core. Positive  $\text{N}_2\text{-N}$  fluxes indicate the net removal of  $\text{N}_2$  likely attributable to dominance of denitrification and anammox, whereas negative  $\text{N}_2\text{-N}$  fluxes indicate production of  $\text{N}_2$  and likely dominance of  $\text{N}_2$  fixation. The same equation was used to calculate dissolved nutrient fluxes for each core.

### Sediment data analysis

Sediment samples were collected from the top 5 cm of each core to analyze differences among OM content, percent C (% C), percent N (% N), and molar C:N ratio. Samples were dried, ground with a Thomas–Wiley Intermediate Mill (Thomas Scientific, Swedesboro, New Jersey), dried at 50 °C to a constant mass, and weighed to estimate dry mass (DM). Ash-free dry mass (AFDM) was measured by combusting a 250-mg subsample at 500 °C for 1 h in a Thermo Scientific Thermolyne muffle furnace (Thermo Fisher Scientific, Waltham, Massachusetts), and subtracting combusted material mass from DM to obtain AFDM (Benfield 2006). Percent OM was calculated as:

$$\%OM = \left( \frac{[\text{sampleDM} - \text{sampleAFDM}]}{[\text{sampleDM}]} \right) \times 100 \quad (3)$$

and used to convert DM to AFDM for whole cores. The nutrient content (% C, % N) of oven-dried (50 °C) material was quantified in a Vario Max CNS

elemental analyzer (Elementar, Mt Laurel, New Jersey), using ground peach leaf standard (NIST SRM 1547) to correct all elemental analyses based on recovery efficiencies. Molar C:N ratios were calculated using % C and % N values.

### Statistical analysis

The influence of sampling date and habitat on sediment OM, % C, % N, and molar C:N ratio was assessed using linear mixed effects modeling (LME) which included random effects (~1core). The restricted maximum likelihood criterion was used to fit all models. Assumptions of all models was assessed visually with normality plots (*qqnorm*) and standardized residual plots across treatments (Zuur et al. 2009). If error variances differed between habitats and dates, this heterogeneity was incorporated by modeling variance separately with the *VarIdent* command (Zuur et al. 2009). The linear mixed effects models were run in the nlme package (Pinheiro et al. 2020). All analyses were run in R (R Core Team 2020).

Generalized additive mixed models (GAMM) were used in two different forms to address our hypotheses. First, a simple GAMM was run to develop different smoothers with time for each habitat type to estimate temporal patterns in sediment fluxes among habitats. Next, a second GAMM was used to specifically identify what measured water column and sediment factors explained significant variability in benthic  $\text{N}_2\text{-N}$  flux estimates across habitats and time. All GAMMs used a random intercept to account for multiple flux estimates from individual cores on different field sampling dates. An autoregressive correlation structure (*corCAR1*) was also tested and incorporated into GAMMs to account for temporal autocorrelation across sampling dates in the models. The *mgcv* package with the restricted maximum likelihood criterion was used to fit all models (Wood 2017). Akaike Information Criterion was used to compare competing models of increasing complexity. Akaike weights (*w<sub>i</sub>*), which are interpreted as the weight of evidence that model *i* is the best approximating model given the data and all candidate models, were calculated for each model and used to identify models that had high probability of explaining the most variability with the least terms (Burnham and Anderson 1998).

Partial effects of each predictor variable on  $N_2$ -N flux were evaluated with effective degrees of freedom (*edf*) values and visually with partial effects plots. When *edf*=1, relationships are linear, and increasing *edf* values indicate increasing nonlinearity. For simple time series GAMMs, predicted flux rates through time were converted to annual flux rates for each habitat type by integrating predicted daily rates (hourly flux  $\times$  24) over time (365 days). This process was performed on 500 random draws from the posterior distributions of GAMMs fitted to flux data through time and across habitats to estimate uncertainty in annual flux rates based on modelled daily rates. The *auc* function was used to integrate positive, negative, and net fluxes over 1 year for each random draw by integrating the area under the curve of each simulated prediction line for all predicted flux rates above 0, below 0, and above and below zero combined. The distribution of integrated values was used to estimate probability distributions for all annual fluxes. Post processing, simulated distributions, and visualization of GAMMs were conducted with the *gratia* package (Simpson 2018).

Habitat delineations, area calculations, and whole lake estimates

Habitat zones including shoreline, cypress, and open water were delineated based on vegetation present.

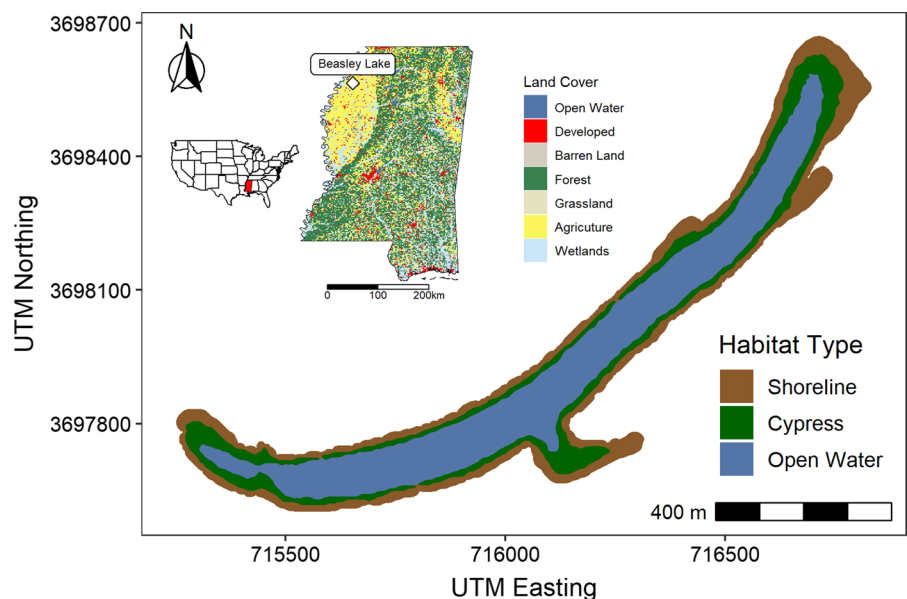
Specifically, shoreline habitat had a depth  $\leq 0.66$  m, cypress habitat had a depth  $> 0.66$  m and  $\leq 1.66$  m, and open water habitat had a depth  $> 1.66$  m. The maximum depth of Beasley Lake was measured at 2.58 m. Maximum depth for each habitat was defined as the deepest depth where habitats no longer overlapped. Each habitat zone was delineated by reclassifying a 1 m resolution bathymetric raster file based on specified habitat depth ranges in R (version 1.3.1093) using the raster package (version 3.4-13) (Hijmans 2021). Spatial data were projected to Universal Transverse Mercator Zone 15 and the area of each habitat zone was calculated using the *area* function in the raster package. Open water habitat represented the largest area at 145,489.91 m<sup>2</sup>, followed by cypress 69,887.54 m<sup>2</sup> and shoreline habitat 49,052 m<sup>2</sup>. The relative area of each habitat zone in Beasley Lake was multiplied by habitat-specific estimated annual flux rates to scale up results to habitat-weighted lake-wide annual net flux estimates for  $N_2$ -N,  $NO_3^-$ -N,  $NH_4^+$ -N, and  $PO_4^{3-}$ -P (Fig. 1).

## Results

### Seasonal patterns in water quality parameters

We observed seasonal patterns in Beasley Lake nutrient and sediment concentrations with winter and

**Fig. 1** Map of study area by habitat type with surrounding land uses



spring characterized by high suspended sediments (SS) and nutrient concentrations and low chlorophyll *a* (Fig. 2). In summer, SS declined with concomitant increases in chlorophyll *a* that corresponded with rapid decreases in availability of  $\text{NO}_3^-$ -N and  $\text{PO}_4^{3-}$ -P that was maintained until late fall (Fig. 2). Total organic C remained between 5 and 10  $\text{mg L}^{-1}$  during the sampling period except for the March 2018 sampling date when the value spiked to near 25  $\text{mg L}^{-1}$  (Fig. 2a). Total Kjeldahl N remained elevated between 0.5 and 2.0  $\text{mg L}^{-1}$  throughout the year (Fig. 2d). A seasonal pattern was observed in TP concentrations with the highest values observed in early to late spring and lowest values nearing zero observed during summer and fall (Fig. 2f).

#### Seasonal and habitat patterns in sediment C and N content

The highest sediment OM content was observed in shoreline habitats except for a brief period during July and August and again in December and January when sediments in cypress habitats had higher OM content (Fig. 3a). Open water sediments had the lowest OM content and were significantly different from shoreline/cypress sediments throughout the study (LMM ANCOVA,  $F_{2, 191}=237.31$ ,  $P<0.0001$ ; Fig. 3a). High values of % C were observed in all habitats during April and May of 2017 (Fig. 3b). The % C in shoreline and cypress habitats was consistently 2–4 -fold higher than in open water (LMM ANCOVA,  $F_{2, 189}=418.51$ ,  $P<0.0001$ ; Fig. 3b). Percent N peaked in April and May 2017 in all habitats and then dropped precipitously for the remainder of the study period (Fig. 3c). Open water habitats also had significantly lower N content than shoreline and cypress habitats (LMM ANCOVA,  $F_{2, 191}=197.51$ ,  $P<0.0001$ ; Fig. 3c). Overall, C:N ratios of shoreline and cypress habitats were higher than in open water (LMM ANCOVA,  $F_{2, 189}=424.25$ ,  $P<0.0001$ ) except for a period during April–May of 2017 (Fig. 3d).

#### Seasonal and habitat patterns in benthic fluxes

Estimated SOD ranged from  $-22$  to  $-73$   $\text{mg m}^2 \text{h}^{-1}$  and while GAMMs did not explain a large amount of variation in SOD through time (*adj. R*<sup>2</sup>=0.29), models did suggest more variation occurred in shoreline habitats (*edf*=11.34,  $F=7.76$ ,

$P<0.001$ ) compared to cypress habitats (*edf*=6.1,  $F=2.65$ ,  $P<0.001$ ), with open water (*edf*=2.79,  $F=0.91$ ,  $P<0.01$ ) exhibiting intermediate levels of variation in seasonal SOD patterns (Online Resource 2). There were also habitat-specific temporal patterns in benthic  $\text{N}_2$ -N flux (Fig. 4a–c). All habitats exhibited higher probability of net positive  $\text{N}_2$ -N flux (dominated by denitrification and/or anammox) from sediments during winter and spring months and periods of net negative  $\text{N}_2$ -N flux (dominated by  $\text{N}_2$  fixation) during the summer, but the magnitude and duration of periods of net positive or negative  $\text{N}_2$ -N flux varied by habitat (Fig. 4a–c). Sediments from shoreline habitats exhibited longer periods of positive flux rates (max  $\text{N}_2$ -N flux = 0.8  $\text{mg m}^2 \text{h}^{-1}$ ) during fall, winter, and spring, and a comparatively short but higher magnitude ( $-1.6$   $\text{mg m}^2 \text{h}^{-1}$ ) period of negative flux during the summer (*edf*=11.39,  $F=13.61$ ,  $P<0.001$ , *adj. R*<sup>2</sup>=0.48; Fig. 4a). Periods of positive  $\text{N}_2$ -N flux from sediments got comparatively shorter and of lower magnitude, whereas the duration of negative  $\text{N}_2$ -N flux periods increased progressively across cypress (*edf*=7.87,  $F=7.2$ ,  $P<0.001$ ; Fig. 4b) and open water habitats (*edf*=4.41,  $F=7.43$ ,  $P<0.001$ ; Fig. 4c).

All habitats exhibited periods of negative benthic  $\text{NO}_3^-$ -N fluxes from sediments during spring but were longer in duration and of greater magnitude in shoreline habitats (*edf*=9.51,  $F=28.01$ ,  $P<0.001$ , *adj. R*<sup>2</sup>=0.58) compared to cypress (*edf*=6.81,  $F=4.16$ ,  $P<0.001$ ) and open water (*edf*=10.04,  $F=13.60$ ,  $P<0.001$ ) habitats. Negative fluxes of  $\text{NO}_3^-$ -N did not occur in any habitat from late spring through early winter (Fig. 4d–f), a period that corresponded with low  $\text{NO}_3^-$ -N availability (Fig. 2). Sediment release of  $\text{NH}_4^+$ -N varied seasonally but positive fluxes occurred across all months for shoreline (*edf*=9.17,  $F=12.12$ ,  $P<0.001$ , *adj. R*<sup>2</sup>=0.49), cypress (*edf*=4.86,  $F=7.68$ ,  $P<0.001$ ), and open water (*edf*=5.43,  $F=4.94$ ,  $P<0.001$ ) habitats with peak  $\text{NH}_4^+$ -N release occurring in July for shoreline (3.9  $\text{mg m}^2 \text{h}^{-1}$ ), cypress and open water habitats (both  $\sim 2.8$   $\text{mg m}^2 \text{h}^{-1}$ ) (Fig. 4g–i). Patterns in  $\text{PO}_4^{3-}$ -P release from sediments were also similar among shoreline (*edf*=7.35,  $F=6.08$ ,  $P<0.001$ , *adj. R*<sup>2</sup>=0.40), cypress (*edf*=5.30,  $F=4.73$ ,  $P<0.001$ ) and open water (*edf*=5.76,  $F=5.01$ ,  $P<0.001$ ) habitats with peak positive fluxes occurring in June–July,



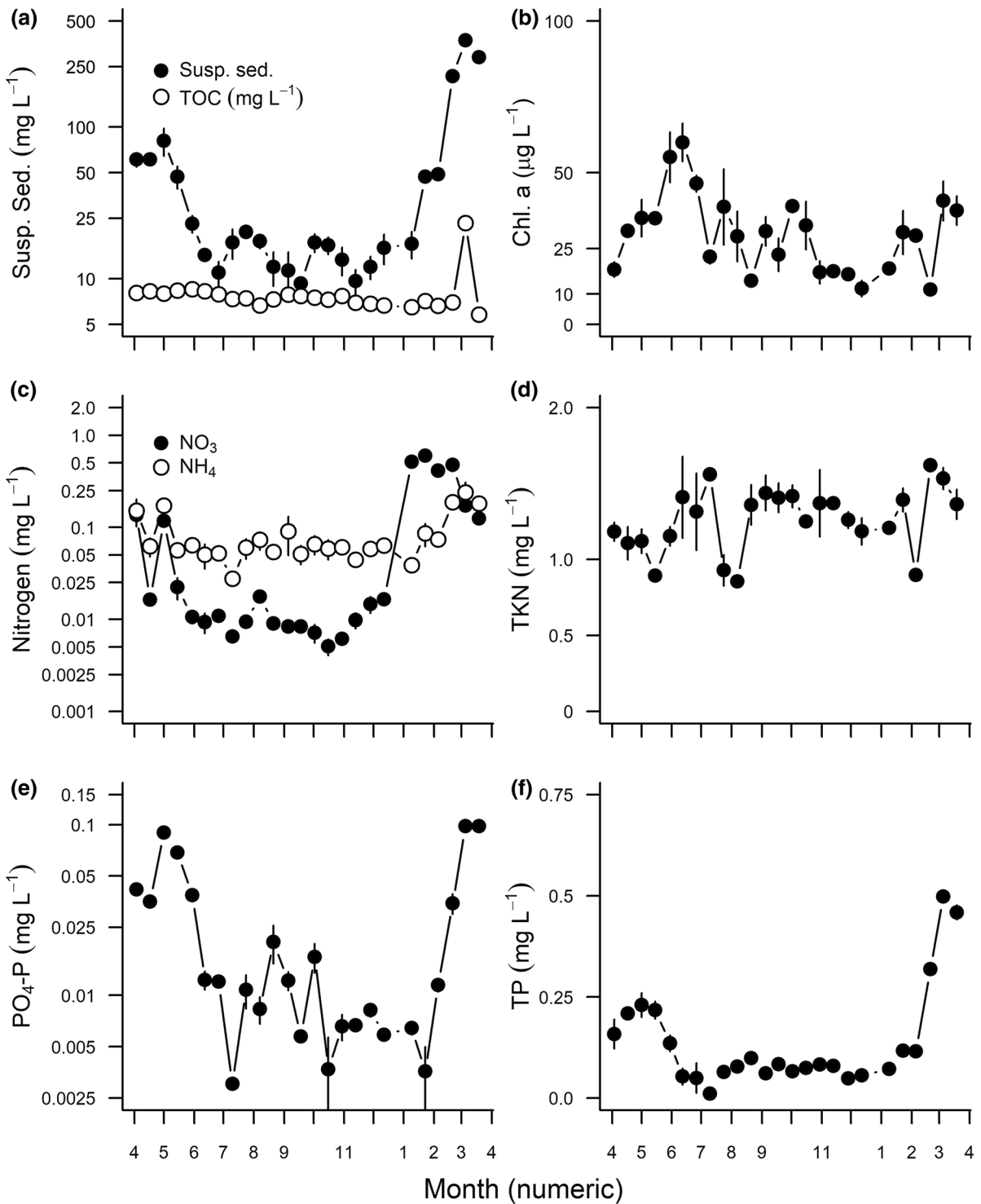
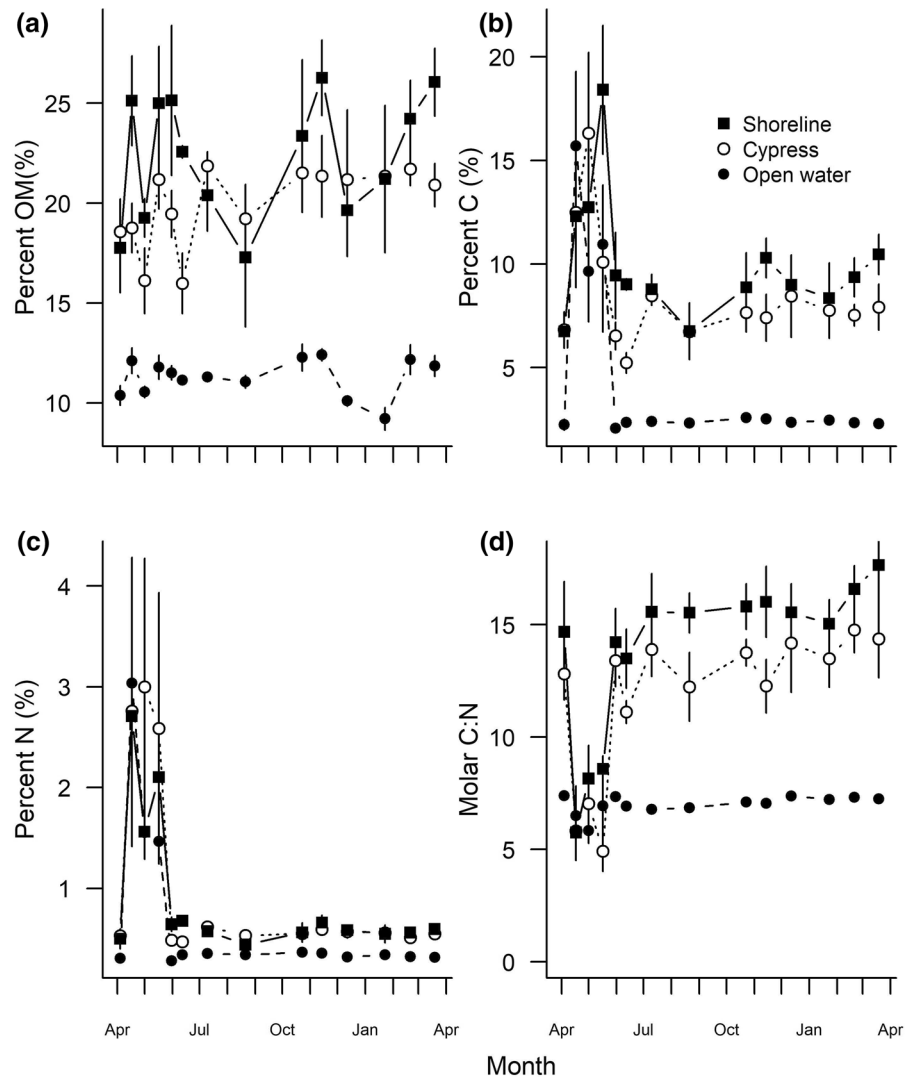


**Fig. 2** Water quality parameters by month in open water habitats. TOC represents total organic carbon, TKN represents Total Kjeldahl Nitrogen, and TP represents Total Phosphorus.

Dots represent means by sampling date with bars representing standard error of the mean

**Fig. 3** Sediment core (a) percent organic matter, (b) percent carbon, (c) percent nitrogen, and (d) molar C:N ratios through time by habitat type. Dots represent means by habitat and sampling date whereas bars show standard error of the mean



no flux during fall and winter, and periods of negative flux starting in February and persisting into early spring (Fig. 4j–l).

The best fit model used all variables across the three habitats, but only explained slightly more variation in benthic  $N_2$ -N flux ( $adj. R^2=0.57$ ) than a simpler model that did not include  $NO_3^-$ -N availability ( $adj. R^2=0.54$ ,  $AICc \Delta_i < 2$ ; Table 1). Despite minimal changes in variance explained, partial effects of individual predictor variables for the highest ranked model provided more insight into habitat specific associations (Fig. 5). Benthic  $N_2$ -N flux was predicted to shift from positive to negative with increasing temperature across all habitats (cypress,  $edf=1.00$ ,  $F=63.4$ ,  $P < 0.001$ ; open

water,  $edf=2.14$ ,  $F=33.1$ ,  $P < 0.001$ ; shoreline habitats,  $edf=3.52$ ,  $F=28.4$ ,  $P < 0.001$ ; Fig. 5a–c). The model predicted a sharp increase in benthic  $N_2$ -N flux at higher levels of SOD in shoreline habitats ( $edf=4.04$ ,  $F=22.7$ ,  $P < 0.001$ ), linear increases with SOD in cypress habitats ( $edf=1.00$ ,  $F=20.4$ ,  $P < 0.001$ ), but there was not a significant relationship with SOD in open water habitats ( $P=0.256$ ; Fig. 5d–f). In shoreline habitats,  $N_2$ -N flux was predicted to increase at lower  $NH_4^+$ -N concentrations before increasing dramatically when concentrations exceeded  $0.12 \text{ mg L}^{-1}$  ( $edf=6.86$ ,  $F=11.9$ ,  $P < 0.001$ ) but was not predicted to respond significantly to increasing  $NO_3^-$ -N ( $P=0.387$ ; Fig. 5g and j). In cypress habitats, the model predicted benthic

**Fig. 4** GAMM predictions for flux rates ( $\text{mg m}^{-2} \text{h}^{-1}$ ) by day for  $\text{N}_2\text{-N}$  within shoreline (a), cypress (b) and open water (c) habitats, and nutrient flux for  $\text{NO}_3\text{-N}$  (d, e, f),  $\text{NH}_4\text{-N}$  (g, h, i), and  $\text{PO}_4\text{-P}$  (j, k, l). Closed circles represent independent core flux measurements, open circles represent average flux for corresponding date. Solid black lines represent GAMM prediction lines and light grey lines represent uncertainty in prediction lines based on 500 random draws from the posterior distribution. Red dashed line represents flux of zero. Estimates were multiplied by 24 h to get daily rates and integrated over 365 days to estimate annual fluxes presented in Table 2

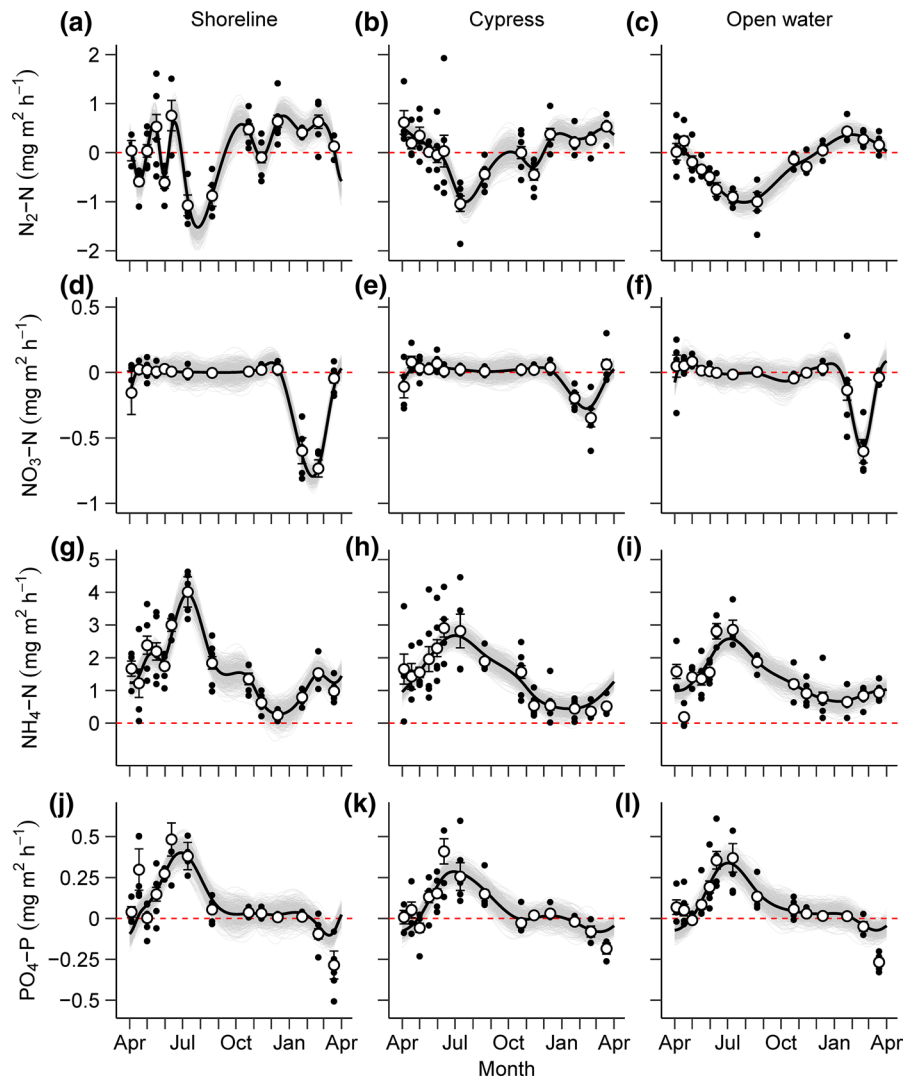
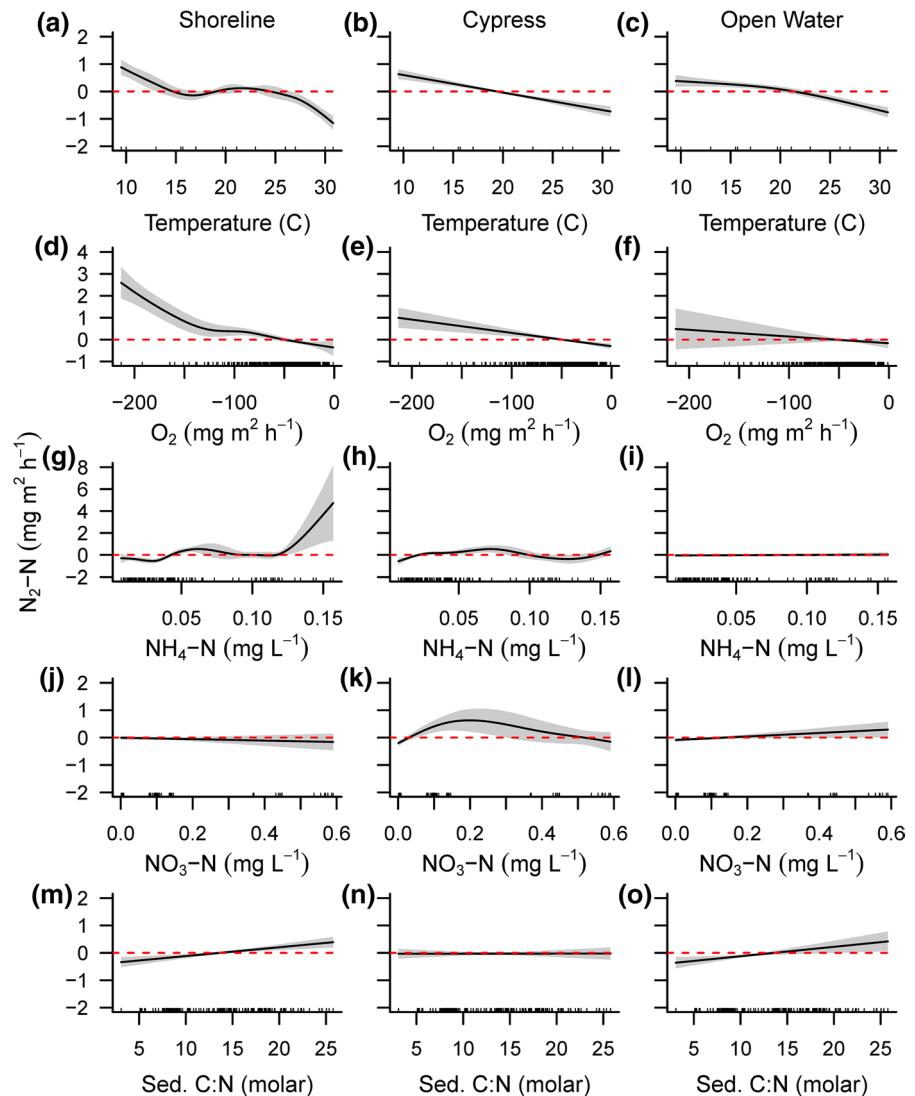


**Table 1** Top ranked GAMMs that predict significant variation in  $\text{N}_2\text{-N}$  flux

Model	Adj. $R^2$	AIC	$\Delta_i$	$w_i$
$\text{N}_2\text{-N flux} \sim s(\text{Temp., by = Habitat}) + s(\text{SOD, by = Habitat}) + s(\text{NH}_4\text{-N, by = Habitat}) + s(\text{NO}_3\text{-N, by = Habitat}) + s(\text{C:N molar, by = Habitat})$	0.57	792.5	0.00	0.648
$\text{N}_2\text{-N flux} \sim s(\text{Temp., by = Habitat}) + s(\text{SOD, by = Habitat}) + s(\text{NH}_4\text{-N, by = Habitat}) + s(\text{C:N molar, by = Habitat})$	0.54	794.2	1.71	0.275
$\text{N}_2\text{-N flux} \sim s(\text{Temp.}) + s(\text{SOD}) + s(\text{NH}_4\text{-N}) + s(\text{C:N molar})$	0.47	798.2	5.69	0.038
$\text{N}_2\text{-N flux} \sim s(\text{Temp.}) + s(\text{SOD}) + s(\text{NH}_4\text{-N}) + s(\text{NO}_3\text{-N}) + s(\text{C:N molar})$	0.48	799.6	7.17	0.018
$\text{N}_2\text{-N flux} \sim s(\text{Temp., by = Habitat}) + s(\text{SOD, by = Habitat}) + s(\text{C:N molar, by = Habitat})$	0.50	800.6	8.16	0.011
$\text{N}_2\text{-N flux} \sim s(\text{Temp.}) + s(\text{SOD}) + s(\text{NH}_4\text{-N}) + s(\text{NO}_3\text{-N})$	0.47	802.9	10.42	0.004
$\text{N}_2\text{-N flux} \sim s(\text{Temp.}) + s(\text{SOD}) + s(\text{NH}_4\text{-N})$	0.45	804.4	11.96	0.002

Ranking based on  $\text{AIC}_c$  values for 36 competing models.  $s$  represents a coefficient for slope. Only models that received a weight ( $w_i$ ) > 0 are presented

**Fig. 5** GAMM results for  $N_2$ -N flux ( $mg\ m^{-2}\ h^{-1}$ ) across habitat types. Plots are partial plots of the smooth terms in the model, and the y axis is the intercept plus the partial effect of the individual smooths. Partial effects of predictor variables on  $N_2$ -N flux include temperature (a, b, c), sediment  $O_2$  (d, e, f),  $NH_4^+$ -N (g, h, i),  $NO_3^-$ -N (j, k, l), and sediment C:N ratio (m, n, o) by habitat. The black solid lines represent the trend line and grey shaded area represents 95% confidence bands



$N_2$ -N flux increases at moderate concentrations of both  $NH_4^+$ -N ( $edf=5.74$ ,  $F=5.90$ ,  $P<0.001$ ) and  $NO_3^-$ -N ( $edf=2.77$ ,  $F=6.41$ ,  $P<0.001$ ; Fig. 5h and k). Water column  $NH_4^+$ -N had no predictive effects on  $N_2$ -N flux in open water habitats ( $P=0.630$ , Fig. 5i), but fluxes were predicted to shift from negative to slightly positive with increasing  $NO_3^-$ -N availability ( $edf=1.00$ ,  $F=5.27$ ,  $P=0.022$ , Fig. 5l). Increasing sediment C:N ratios were correlated with increasing  $N_2$ -N fluxes in shoreline ( $edf=1.00$ ,  $F=16.57$ ,  $P<0.001$ ) and open water habitats

( $edf=1.00$ ,  $F=7.87$ ,  $P<0.01$ ), but not cypress habitats ( $P=0.973$ ; Fig. 5m–o).

#### Estimated annual fluxes

Seasonal patterns in benthic flux rates, based on the integration of predicted rates from simple habitat specific time series GAMMs (Fig. 4), revealed large differences among habitat specific contributions to annual  $N_2$ -N flux contributions (Table 2). Positive net annual  $N_2$ -N fluxes (median= $0.26\ g\ m^{-2}\ Y^{-1}$ ) were confined to shoreline habitats only, while the dominant habitat (open water) had large negative

**Table 2** Median and 95% confidence intervals for annual benthic fluxes from Beasley Lake sediments calculated from cores ( $\text{g m}^{-2} \text{Y}^{-1}$ ) and whole lake extrapolated fluxes ( $\text{kg Y}^{-1}$ )

Habitat	Flux (+)	Flux (-)	Net flux	Whole lake
<i>N<sub>2</sub>-N</i>				
Shoreline	2.42 (1.98, 2.89)	-2.17 (-2.57, -1.83)	0.26 (-1.75, 0.70)	12.75 (-85.84, 34.34)
Cypress	1.46 (1.14, 1.78)	-1.67 (-2.16, -1.23)	-0.22 (-0.63, 0.16)	-15.37 (-44.03, 11.18)
Open water	0.74 (0.42, 1.06)	-3.08 (-3.50, -2.68)	-2.34 (-2.65, -2.05)	-340.44(-385.55, -298.25)
<i>NO<sub>3</sub>-N</i>				
Shoreline	0.17 (0.10, 0.28)	-1.16 (-1.29, -1.06)	-0.99 (-1.13, -0.85)	-48.56 (-55.43, -41.69)
Cypress	0.19 (0.11, 0.32)	-0.42 (-0.54, -0.32)	-0.22 (-0.35, -0.11)	-15.37 (-24.46, -7.69)
Open water	0.20 (0.12, 0.29)	-0.65 (-0.81, -0.55)	-0.46 (-0.59, -0.34)	-66.92 (-85.84, -49.47)
<i>NH<sub>4</sub>-N</i>				
Shoreline	14.40 (13.69, 15.10)	0.00 (-0.10, 0.00)	14.40 (13.69, 15.10)	706.35 (671.53, 740.69)
Cypress	12.46 (11.86, 13.06)	0.00 (0.00, 0.00)	12.46 (11.86, 13.06)	870.80 (828.89, 912.73)
Open water	12.00 (11.42, 12.49)	0.00 (0.00, 0.00)	12.00 (11.42, 12.49)	1745.88 (1661.49, 1817.17)
<i>PO<sub>4</sub>-P</i>				
Shoreline	0.91 (0.78, 1.06)	-0.12 (-0.21, -0.05)	0.80 (0.66, 0.94)	39.24 (32.37, 46.11)
Cypress	0.71 (0.57, 0.87)	-0.17 (-0.29, -0.08)	0.54 (0.41, 0.66)	37.74 (28.65, 46.13)
Open water	0.85 (0.69, 0.99)	-0.12 (-0.21, -0.04)	0.73 (0.60, 0.84)	106.21 (87.29, 122.21)

Positive net fluxes for  $\text{N}_2\text{-N}$  represent removal of N from the lake; negative net fluxes for  $\text{NO}_3\text{-N}$  also represent removal. Conversely, positive net fluxes for  $\text{NH}_4\text{-N}$  represent contribution of N to Beasley Lake

annual fluxes (median =  $-2.34 \text{ g m}^{-2} \text{ Y}^{-1}$ ). Cypress habitats had slightly negative net annual  $\text{N}_2\text{-N}$  flux (median =  $-0.22 \text{ g m}^{-2} \text{ Y}^{-1}$ ). Separately integrating positive and negative fluxes revealed that differences in net fluxes between shoreline and cypress habitats were driven by higher annual positive fluxes in shoreline habitats (Table 2). Annual positive flux rates ranged from  $0.74 \text{ g m}^{-2} \text{ Y}^{-1}$  (open water) to  $2.42 \text{ g m}^{-2} \text{ Y}^{-1}$  (shoreline), with rates increasing by approximately 97% as habitat shifted from open water to cypress, and by 227% when comparing open water to shoreline habitats. In contrast, annual negative flux estimates were similar between shoreline and cypress habitats with overlapping probability distributions and were on average, 38% lower ( $1.67 \text{ g m}^{-2} \text{ Y}^{-1}$  and  $2.17 \text{ g m}^{-2} \text{ Y}^{-1}$  for cypress and shoreline habitats respectively) than estimated negative flux rates observed in open water habitats ( $3.08 \text{ g m}^{-2} \text{ Y}^{-1}$ ; Table 2). Weighting rates by habitat distribution and extrapolating to whole lake estimates indicate Beasley Lake sediments accumulate  $343.06 \text{ kg}$  of N annually through the net effects of benthic  $\text{N}_2\text{-N}$  flux (Table 2).

Seasonal patterns in dissolved inorganic nutrient fluxes integrated across time also revealed differences in annual fluxes among habitats (Table 2).

All habitats were net sinks for  $\text{NO}_3\text{-N}$  but annual uptake in shoreline habitat ( $-0.99 \text{ g m}^{-2} \text{ Y}^{-1}$ ) exceeded cypress ( $-0.22 \text{ g m}^{-2} \text{ Y}^{-1}$ ) and open water ( $-0.46 \text{ g m}^{-2} \text{ Y}^{-1}$ ) habitats in Beasley Lake by 78 and 54%, respectively (Table 2). All habitats were also a source of  $\text{NH}_4\text{-N}$  over the course of a year, and rates were similar among cypress ( $12.46 \text{ g m}^{-2} \text{ Y}^{-1}$ ) and open water ( $12.00 \text{ g m}^{-2} \text{ Y}^{-1}$ ) habitats, but shoreline habitats ( $14.40 \text{ g m}^{-2} \text{ Y}^{-1}$ ) had 16–20% higher rates of annual  $\text{NH}_4\text{-N}$  flux from sediments to the water column (Table 2). After accounting for all DIN fluxes, we estimated Beasley Lake sediments are a source of N with shoreline, cypress and open water habitats contributing  $13.41$ ,  $12.24$  and  $11.54 \text{ g m}^{-2} \text{ Y}^{-1}$  of N to the water column. Similarly, sediments across all habitats were a source of  $\text{PO}_4\text{-P}$  to the lake annually. Estimated annual fluxes from shoreline ( $0.80 \text{ g m}^{-2} \text{ Y}^{-1}$ ) and open water ( $0.73 \text{ g m}^{-2} \text{ Y}^{-1}$ ) habitats which were on average, 42% greater than estimated annual rates from cypress habitats. When rates were weighted by habitat area and extrapolated to whole lake estimates, results indicate Beasley Lake sediments are a sizeable source of N and P to the water column, only removing  $130.86 \text{ kg NO}_3\text{-N Y}^{-1}$  through sediment

uptake while releasing 3323.03 kg of  $\text{NH}_4^+$ -N and 183.19 kg of  $\text{PO}_4^{3-}$ -P annually (Table 2).

## Discussion

Our results demonstrate significant spatial and temporal variability in sediment nutrient fluxes in Beasley Lake. Sediment  $\text{N}_2$ -N flux indicated that  $\text{N}_2$  losses from the lake were highest during the winter and spring when  $\text{NO}_3^-$ -N availability was greatest, particularly in shoreline habitats. However, fluxes of  $\text{N}_2$ -N from the water column and incorporation into sediments during the summer balanced or in some cases exceeded  $\text{N}_2$  losses during the winter and spring. This has been observed in other lakes where algal bloom-fueled N deposition has been found to favor internal recycling over denitrification driven  $\text{N}_2$  losses (Yao et al. 2018; Albert et al. 2021). In addition to algal N deposition, heterotrophic bacteria can opportunistically fix  $\text{N}_2$  when the energetic costs of fixation are lowered in sediments (Yao et al. 2018). Our annual  $\text{N}_2$ -N flux estimates weighted by habitat area indicate that  $\text{N}_2$ -N exchange is a net source of atmospheric N to Beasley Lake sediments and the balance of sediment  $\text{NO}_3^-$ -N uptake in the spring and  $\text{NH}_4^+$ -N release peaking in the summer suggest that sediments are an important site for recycling sources of allochthonous and autochthonous N to the water column. Likewise, Beasley Lake sediments also served as an internal net source of dissolved P to the water column. Taken together, our results suggest that internal mechanisms occurring in sediments can be a significant source of inorganic nutrients to oxbow lakes that is on the same order of magnitude as runoff-generated nutrient inputs from agricultural watersheds within the study region. Management practices designed to reduce eutrophication in shallow oxbow lakes need to account for a legacy of agricultural inputs that may impact N and P availability during algal bloom conditions indirectly through influencing  $\text{N}_2$  fixation and directly through sediment release.

### Drivers of $\text{N}_2$ -N flux in Beasley Lake

In this study, our flow-through sediment core incubations were designed to measure overall  $\text{N}_2$  production and therefore only provide information on “net” denitrification. Net denitrification is the difference

between gross denitrification plus other  $\text{N}_2$  producing processes (coupled nitrification–denitrification, anammox) and gross N fixation (Groffman et al. 2006). More in-depth incubation techniques relying on recent iterations of the isotope pairing technique (IPT) or  $^{30}\text{N}_2$  incubations, combined with modelling can help quantify the specific roles of different processes driving  $\text{N}_2$ -N fluxes from benthic sediments (Groffman et al. 2006; Trimmer et al. 2006; Crowe et al. 2012; Newell et al. 2016b). Denitrification is an important component of N removal in lakes (Saunders and Kalff 2001) that is influenced not only by the abundance of denitrifying bacteria but also physicochemical rate-limiting factors including the availability and quality of OM, oxidation status, available N, light, temperature, pH (Knowles 1982; Seitzinger 1988; Nielsen et al. 1990; Arango et al. 2007; Burgin and Hamilton 2007; Vymazal 2007), and longer hydrologic residence times (Findlay et al. 2013). It is plausible to assume denitrification is the dominant process during periods of high positive  $\text{N}_2$ -N flux across habitats, given this corresponded with periods of higher  $\text{NO}_3^-$ -N availability and was most associated with shoreline habitats where OM was highest. However, GAMM partial smoothers identified decreasing temperature, higher  $\text{O}_2$  consumption, and higher C:N ratios as significant predictors of greater  $\text{N}_2$ -N flux in edge habitats but did not identify  $\text{NO}_3^-$ -N as a significant predictor. Denitrification typically peaks during summer if not limited by N availability (Pina-Ochoa and Álvarez-Cobelas 2006; David et al. 2006) but high rates can also occur during winter when N is most available if temperature is not limiting (Arango and Tank 2008). Our results support that  $\text{N}_2$ -N flux was negatively correlated with temperature and positive rates occurred during cooler months. This is likely because periods of high temperature also correspond with periods of high demand and plausible N limitation or could indicate that anammox contributes significantly to  $\text{N}_2$ -N flux in our system. Land–water interfaces can be hotspots of anammox activity (Zhu et al. 2013) and within shoreline habitat zones examined in this study,  $\text{N}_2$ -N flux was predicted to increase dramatically when  $\text{NH}_4^+$ -N exceeded  $0.1 \text{ mg L}^{-1}$ , which corresponds with periods of peak  $\text{N}_2$ -N flux in spring. Anammox activity also declines at temperatures above  $25 \text{ }^\circ\text{C}$  which may explain the lack of positive  $\text{N}_2$  flux despite high  $\text{NH}_4^+$ -N fluxes from sediments during the summer

(Tan et al. 2020). We cannot rule out that higher  $N_2$ -N fluxes in edge habitats during the spring may have been driven or at least influenced by anammox. Regardless of the particular pathway, our results demonstrate  $N_2$  loss from Beasley Lake is primarily restricted to lake edge habitats and limited to periods of high inorganic N availability.

Despite specific periods of positive  $N_2$ -N fluxes within discrete habitats, negative  $N_2$ -N fluxes were the dominant pattern both spatially and temporally within Beasley Lake. Negative  $N_2$ -N fluxes can indicate that  $N_2$  fixation, the process by which  $N_2$  is converted to  $NH_4^+$ -N, is exceeding both denitrification and anammox in benthic sediments (Fulweiler et al. 2013). Negative  $N_2$ -N fluxes dominated in this study, ranging from  $-0.02$  to  $-1.86$   $mg\ m^{-2}\ h^{-1}$ , and represent the low end of previously reported negative fluxes from freshwater environments using similar methods (Scott et al. 2008; Grantz et al. 2012). Estuarine studies using similar methods have reported even higher negative fluxes ranging from  $-9.1$  to  $-11.28$   $mg\ m^{-2}\ h^{-1}$ , indicating  $N_2$  fixation can be an important contributor to ecosystem N cycling (Fulweiler et al. 2007; Viellard and Fulweiler 2012).  $N_2$  fixation was not directly measured in this study; however, low  $NO_3^-$ -N conditions and net  $N_2$  consumption support the role of  $N_2$  fixation in contributing to patterns of  $N_2$ -N flux in Beasley Lake. Free living cyanobacteria are primarily responsible for  $N_2$  fixation in lakes, but bacteria with *nifH* (a gene associated with  $N_2$  fixation) are ubiquitous in benthic environments, indicating high probabilities for sediment  $N_2$  fixation in aquatic ecosystems (Newell et al. 2016b). Given the low light environment of benthic zones in eutrophic lakes, fixation in these environments is likely facilitated by heterotrophic, chemolithotrophic, chemoorganotrophic bacteria and archaea, particularly as anoxia in the top layer of sediments reduces the energetic costs of  $N_2$  fixation (Beman et al. 2012; Yao et al. 2018). Recent studies have demonstrated that dissolved inorganic N-enriched environments such as eutrophic lakes do not necessarily inhibit  $N_2$  fixation; instead, factors that explained fluxes in our study, including temperature, organic C, and oxygen, may regulate patterns of  $N_2$  fixation in benthic sediments (Knapp 2012; Bertics et al. 2013; McCarthy et al. 2016; Newell et al. 2016a).

$N_2$ -N flux rates within Beasley Lake range from net negative ( $-1.86$ ) to net positive fluxes

( $2.35$   $mg\ m^{-2}\ h^{-1}$ ) across all habitats (Fig. 4a–c). Other oxbow lake studies report ranges of  $0.101$  to  $0.18$   $mg\ m^{-2}\ h^{-1}$  (Harrison et al. 2012) and rates from an agriculturally influenced lake study ranged between  $0.036$  and  $2.46$   $mg\ m^{-2}\ h^{-1}$  (Bruesewitz et al. 2011). Compared to estimates from a freshwater marsh complex, positive rates in Beasley Lake were similar ( $2.35$  vs.  $2.58$   $mg\ N\ m^{-2}\ h^{-1}$ , Scott et al. 2008) while negative rates, presumably driven by  $N_2$  fixation, were lower ( $-1.86$  vs.  $-3.78$   $mg\ N\ m^{-2}\ h^{-1}$ , Scott et al. 2008). Ullah and Faulkner (2006) recorded denitrification rates of up to  $0.2096$   $mg\ N\ m^{-2}\ h^{-1}$  in agricultural fields and  $1.062$   $mg\ N\ m^{-2}\ h^{-1}$  in forested wetlands within the Beasley Lake watershed. Other freshwater wetland systems have reported average rates of up to  $2.5$   $mg\ m^{-2}\ h^{-1}$  (Poe et al. 2003). When compared to previously published rates, our observed rates represent a similar magnitude and range of net  $N_2$ -N fluxes compared to studies that employed seasonal sampling. Seasonal shifts between periods of light limitation by high SS and DIN availability in winter and spring, and periods of high chlorophyll *a*, and low DIN availability during summer and fall (Lizotte et al. 2014, 2017; Wren et al. 2019), as well as strong partitioning of factors controlling  $N_2$ -N flux among discrete habitats, drive the wide variety of  $N_2$ -N flux rates observed in this study and suggest that Beasley Lake is dynamic in its N processing capacity.

#### Role of internal loading from sediments in Beasley Lake

Release of N and P from lake sediments are often coupled, particularly in shallow eutrophic lakes, with nutrient release driven by interrelated factors including the prevalence and duration of anoxic conditions, temperature, and stratification status (Katsev et al. 2006; Li et al. 2016; Gibbons and Bridgeman 2020). In warmer months, thermal stratification prevents the physical mixing of oxygenated surface water with bottom water resulting in anoxic benthic conditions which can be exacerbated by seasonal and global change (North et al. 2014; Kraemer et al. 2015). Beasley temperatures were similar among habitats for a given sampling date but varied substantially through seasons (Online Resource 1). Elevated temperatures can stimulate fluxes by increasing mineralization and diffusion rates as well as lowering of redox potential

via increased microbial activity (Katsev et al. 2006; Anthony and Lewis 2012; Small et al. 2014). This study observed negative  $\text{NO}_3^-$ -N flux rates during periods of elevated  $\text{NO}_3^-$ -N concentrations and no flux during periods of low  $\text{NO}_3^-$ -N availability, similar to reports from lakes with episodic nutrient delivery where sediment nutrient recycling can drive productivity (Fig. 4d–f; McCarthy et al. 2007; 2016). Nitrate fluxes may also be evidence of dissimilatory nitrate reduction to ammonium (DNRA) which has been found to dominate in relatively high labile C, low  $\text{NO}_3^-$ -N systems (Tiedje 1988). The balance between DNRA and denitrification can also be influenced by oxidation state with anoxic conditions favoring obligate anaerobes involved in DNRA over facultative aerobic denitrifiers (Matheson et al. 2002). It is plausible that a portion of the  $\text{NO}_3^-$ -N uptake observed in our study could be associated with DNRA given that we observed  $\text{NH}_4^+$ -N fluxes throughout the study. However,  $\text{NH}_4^+$ -N fluxes can also occur through the direct mineralization of OM. We observed positive fluxes throughout the study, but  $\text{NH}_4^+$ -N fluxes peaked ( $>4 \text{ mg N m}^{-2} \text{ h}^{-1}$ ) in July when temperature and SOD were greatest, similar to other peak fluxes observed in Mississippi River Basin ( $3.90 \text{ mg N m}^{-2} \text{ h}^{-1}$ ; Li et al. 2020). Peak  $\text{NH}_4^+$ -N flux rates also corresponded with a period after chlorophyll *a* had peaked and was declining and represented a period of high OM deposition (Wren et al. 2019). Experimental additions of seston to lake sediments demonstrate that seston deposition stimulates SOD,  $\text{NH}_4^+$ -N, and P fluxes by providing a source of organic N and P for mineralization (Østergaard and Jensen 1992). James (2010) measured  $\text{NH}_4^+$ -N fluxes under anoxic conditions of  $2.34 \text{ mg N m}^{-2} \text{ h}^{-1}$  in lake complexes of the Upper Mississippi River Basin consistent with rates observed in this study during spring and late fall. P fluxes in a Delta oxbow lake reached up to  $4.0 \text{ mg m}^{-2} \text{ h}^{-1}$  (Evans et al. 2021). In this study, maximum flux rates for P were  $2.97 \text{ mg P m}^{-2} \text{ h}^{-1}$  which is consistent with previously reported rates for eutrophic reservoir sediments incubated under aerobic conditions ( $1.03$  to  $4 \text{ mg}$ ; Haggard et al. 2005; Haggard and Soerens 2006), lower than reports for anaerobic conditions ( $4.4$  to  $15 \text{ mg P m}^{-2} \text{ h}^{-1}$ ; Haggard et al. 2005; Haggard and Soerens 2006) but much higher than rates observed in less directly impacted lakes ( $0.07 \text{ mg P m}^{-2} \text{ h}^{-1}$ ; Sen et al. 2007). Song and Burgin (2017) demonstrate

that eutrophication can amplify biological control of internal phosphorus loading in agricultural lakes because P loading in hypereutrophic lakes may be stimulated by organic matter breakdown and extracellular enzyme activity under aerobic conditions in addition to anaerobic Fe–P release. While more work on the specific controls of P release from oxbow lake sediments is needed, this study demonstrates that sediment P fluxes were positive across all habitats (Fig. 4), supporting the role of internal P loading in sustaining eutrophic conditions in agriculturally influenced oxbow lakes.

In Beasley Lake, external nutrient supply varies over the course of a year with lower runoff inputs in summer compared to fall, winter, and spring (Locke et al. 2020). Beginning in the fall, as precipitation increases, rising nutrient levels are observed (Fig. 2) which may contribute to the peak positive  $\text{N}_2$ -N flux rates observed in all habitats (Fig. 4 b). Following the fall and winter periods, precipitous reductions in  $\text{PO}_4^{3-}$ -P, TP, and  $\text{NO}_3^-$ -N are also observed at the beginning of summer (June; Fig. 2a, c, d). Previous studies in other systems indicate increasing chlorophyll *a* levels are associated with non-limiting N and P conditions and initiate subsequent internal cycling of coupled nitrification and denitrification (Reynolds 1998, 1999; An and Joye 2001; Chorus and Spijkerman 2021). Rising chlorophyll *a* levels coupled with observed declines in dissolved inorganic nutrients in Beasley Lake, during early summer signal the initiation of a period of internal nutrient release and cycling (Fig. 2). Multidimensional numerical models applied to a nearby Delta oxbow identified internal sediment fluxes as important drivers of chlorophyll *a* in these systems (Chao et al. 2006; 2010) and Haggard et al. (2005) estimated that internal P loading can represent as much as 25% of the external load to eutrophic reservoirs in Oklahoma. An episodic, allochthonous nutrient pulse driven by runoff effectively primes the pump for legacy nutrients to sustain productivity within Beasley Lake (King et al. 2017). Recent projections of external nutrient loads to Beasley Lake estimate 2312.5 kg TN and 625 kg TP are added each year when planted in soybeans following business-as-usual management (Yasarer et al. 2017). Our estimates of whole lake internal loads are relatively similar ( $3139.84 \text{ kg N Y}^{-1}$ ,  $183.19 \text{ kg P Y}^{-1}$ ). It is not clear whether Beasley Lake is able to process these external loads, nor whether the lake has



shifted from sink to source over time. Several factors including climate change and crops requiring high fertilizer inputs are anticipated to increase external loading (Yasarer et al. 2017; Paerl et al. 2020), exacerbating eutrophication within shallow agricultural lakes such as Beasley Lake. Determining the age of sediments and associated nutrients being mineralized may be helpful in identifying whether BMPs are still effective and estimating how long legacy nutrients are taking to be processed in Beasley Lake (Song et al. 2017). Additionally, this study was conducted while soybean cultivation was the primary agronomic practice within the watershed. Additional information on oxbow lake biogeochemical cycling under the influence of different crop rotations, such as maize which can generate higher N runoff loads, are needed to provide more insight into the role of agricultural-influenced oxbow lakes as nutrient source or sinks within the MAP landscape.

## Conclusions

We hypothesized that oxbow lakes would serve as N sinks in the MAP due to their polymictic structure, ability to store and trap carbon, relatively long hydraulic residence time, and high N inputs. Despite strong potential for oxbow lakes in agricultural landscapes to serve as nutrient sinks, we found that annual internal N release rates from lake sediments can match or exceed expected loading of N from agricultural watersheds planted in soy over a given growing season. Internal P loading may also contribute significantly to maintaining eutrophic conditions in oxbow lakes. Our findings suggest legacy nutrients are cycling at rates equal in magnitude to watershed loading rates which may help to explain why the implementation of BMPs has not resulted in significant TN reduction in the Beasley Lake Watershed (Lizotte et al. 2017). With reduced external loads, rates of nutrient processing may change (Sas 1989; Jeppensen et al. 2005). To anticipate how rates may change, a better understanding of the interplay between autochthonous production and allochthonous inputs of OM production in space and through time would be a beneficial area of future research. Furthermore, more research into the extent of anoxia changes with depth and mixing within the lake could help to inform land management decisions. Our results highlight the

significance of internal nutrient loading potential in regulating biogeochemical processes within understudied oxbow lake ecosystems. Given the prevalence of oxbow lakes in large river alluvial floodplain drainage networks, which are increasingly dominated by row crop agriculture globally, more research into the complexities of biogeochemical cycling within them is essential to improving management and recovery from eutrophication in these systems.

**Acknowledgments** We would like to thank Sam Testa, Terry Welch, Wade Steinreide, Mark Griffith, Lisa Brooks, James Hill, Tate Hillhouse, and James Gledhill for assisting in data collection and sample processing. Lindsey Yasarer provided data to establish habitat zone areas and participated in discussions which greatly improved this manuscript. Tim Strickland, Cliff Ochs, and two anonymous reviewers provided much appreciated comments which improved an earlier draft of this manuscript. Mention of trade names or commercial products in this article is solely for the purpose of providing specific information and does not imply recommendation or endorsement by the US Department of Agriculture. The US Department of Agriculture is an equal opportunity employer and provider.

**Authors contributions** Conceptualization: RLN and JMT; Methodology: RLN and JMT; Formal analysis and investigation: RLN, JMT, and SED; Writing—original draft preparation: RLN; Writing—reviewing and editing: RLN, JMT, and SED.

**Funding** This research was supported by the US Department of Agriculture, Agricultural Research Service.

**Data availability** Available upon request to corresponding author.

**Code availability** Not applicable.

## Declarations

**Conflict of interest** The authors declare no conflict of interest pertaining to the content of this article.

## References

- Albert S, Bonaglia S, Stjärnkvist N, Winder M, Thamdrup B, Nascimento FJA (2021) Influence of settling organic matter quantity and quality on benthic nitrogen cycling. *Limnol Oceanogr* 66:1882–1895. <https://doi.org/10.1002/lno.11730>
- An S, Joye SB (2001) Enhancement of coupled nitrification-denitrification by benthic photosynthesis in shallow estuarine sediments. *Limnol Oceanogr* 46:62–74
- Anthony JL, Lewis WM Jr (2012) Low boundary layer response and temperature dependence of nitrogen and

- phosphorus releases from oxic sediments of an oligotrophic lake. *Aquat Sci* 74:611–617
- APHA (American Public Health Association) (2005) Standard Methods for the Analysis of Water and Wastewater, 21<sup>st</sup> ed. American Public Health Association, American Water Works Association, & Water Environment Federation, Washington, DC
- Arango CP, Tank JL (2008) Land use influences the spatiotemporal controls on nitrification and denitrification in headwater streams. *J N Am Benthol Soc* 27:90–107
- Arango CP, Tank JL, Schaller JL, Royer TV, Bernot MJ, David MB (2007) Benthic organic carbon influences denitrification in streams with high nitrate concentration. *Freshw Biol* 52:1210–1222
- Beman JM, Popp BN, Alford SE (2012) Quantification of ammonia oxidation rates and ammonia-oxidizing archaea and bacteria at high resolution in the Gulf of California and eastern tropical North Pacific Ocean. *Limnol Oceanogr* 57:711–726. <https://doi.org/10.4319/lo.2012.57.3.0711>
- Benfield EF (2006) Decomposition of leaf material. In: Hauer FR, Lamberti GA (eds) *Methods in Stream Ecology*. Academic Press, San Diego, pp 711–720
- Bertics VJ, Scher CRL, Salonen I, Dale AW, Gier J, Schmitz RA, Treude T (2013) Occurrence of benthic microbial nitrogen fixation coupled to sulfate reduction in the seasonally hypoxic Eckernförde Bay, Baltic Sea. *Biogeochemistry* 10:1243–1258. <https://doi.org/10.5194/bg-10-1243-2013>
- Bruesewitz DA, Hamilton DP, Schipper LA (2011) Denitrification potential in lake sediment increases across a gradient of catchment agriculture. *Ecosystems* 14:341–352
- Burger DF, Hamilton DP, Pilditch CA (2008) Modelling the relative importance of internal and external nutrient loads on water column nutrient concentrations and phytoplankton biomass in a shallow polymictic lake. *Ecol Modell* 211:411–423
- Burgin AJ, Hamilton SK (2007) Have we overemphasized the role of denitrification in aquatic ecosystems? A review of nitrate removal pathways. *Front Ecol Environ* 5:89–96
- Burnham KP, Anderson DR (1998) Practical use of the information-theoretic approach. In: *Model Selection and Inference*. Springer, New York. [https://doi.org/10.1007/978-1-4757-2917-7\\_3](https://doi.org/10.1007/978-1-4757-2917-7_3)
- Buttle JM, McDonald DJ (2002) Coupled vertical and lateral preferential flow on a forested slope. *Water Resour.* <https://doi.org/10.1029/2001WR000773>
- Chao X, Jia Y, Cooper CM, Shields FD Jr, Wang SSY (2006) Development and application of a phosphorus model for a shallow oxbow lake. *J Environ Eng* 132:1498–1507
- Chao X, Jia Y, Shields FD Jr, Wang SSY, Cooper CM (2010) Three-dimensional numerical simulation of water quality and sediment-associated processes with application to a Mississippi Delta lake. *J Environ Manage* 91:1456–1466
- Cheng FY, Basu NB (2017) Biogeochemical hotspots: role of small water bodies in landscape nutrient processing. *Water Resour Res* 53:5038–5056
- Chorus I, Spijkerman E (2021) What Colin Reynolds could tell us about nutrient limitation, N: P ratios and eutrophication control. *Hydrobiologia* 848:95–111
- Crowe SA, Canfield DE, Mucci A, Sundby B, Maranger R (2012) Anammox, denitrification and fixed-nitrogen removal in sediments from the Lower St. Lawrence Estuary. *Biogeochemistry* 9:4309–4321. <https://doi.org/10.5194/bg-9-4309-2012>
- David MB, Wall LG, Royer TV, Tank JL (2006) Denitrification and the nitrogen budget of a reservoir in an agricultural landscape. *Ecol Appl* 16:2177–2190
- Doi H (2009) Spatial patterns of autochthonous and allochthonous resources in aquatic food webs. *Popul Ecol* 51:57–64. <https://doi.org/10.1007/s10144-008-0127-z>
- Duncan JM, Groffman PM, Band LE (2013) Towards closing the watershed nitrogen budget: spatial and temporal scaling of denitrification. *JGR Biogeochemistry* 118:1105–1119. <https://doi.org/10.1002/jgrg.20090>
- Evans JL, Murdock JN, Taylor JM, Lizotte RE Jr (2021) Sediment nutrient flux rates in a shallow, turbid lake are more dependent on water quality than lake depth. *Water* 13:1344. <https://doi.org/10.3390/w13101344>
- Findlay JC, Small GE, Sterner RW (2013) Human influences on nitrogen removal in lakes. *Science* 342:247–250
- Forsberg C (1989) Importance of sediments in understanding nutrient cycling in lakes. *Hydrobiologia* 176–177:263–277
- Fulweiler RW, Nixon SW, Buckley BA, Granger SL (2007) Reversal of the net dinitrogen gas flux in coastal marine sediments. *Nature* 448:180–182. <https://doi.org/10.1038/nature05963>
- Fulweiler RW, Brown SM, Nixon SW, Jenkins BD (2013) Evidence and a conceptual model for the co-occurrence of nitrogen fixation and denitrification in heterotrophic marine sediments. *Mar Ecol Prog Ser* 482:57–68
- Gardner WS, McCarthy MJ, An S, Sobolev D, Sell KS, Brock D (2006) Nitrogen fixation and dissimilatory nitrate reduction to ammonium (DNRA) support nitrogen dynamics in Texas estuaries. *Limnol Oceanogr* 51:558–568
- Gardner WS, Newell SE, McCarthy MJ, Hoffman DK, Lu K, Lavrentyev PJ, Hellweger FL, Wilhelm SW, Liu Z, Bruesewitz DA, Paerl HW (2017) Community biological ammonium demand: a conceptual model for cyanobacteria blooms in eutrophic lakes. *Environ Sci Technol* 51:7785–7793
- Gibbons KJ, Bridgeman TB (2020) Effect of temperature on phosphorus flux from anoxic western Lake Erie sediments. *Water Res* 182:116022
- Grantz EM, Kogo A, Scott JT (2012) Partitioning whole-lake denitrification using in situ dinitrogen gas accumulation and intact sediment core experiments. *Limnol Oceanogr* 57:525–535
- Haggard BE, Soerens TS (2006) Sediment phosphorus release at a small impoundment on the Illinois river, Arkansas and Oklahoma. *USA Eco Eng* 28:280–287
- Groffman PM, Altabet MA, Böhlke JK, Butterbach-Bahl K, David MB, Firestone MK, Giblin AE, Kana TM, Nielsen LP, Voytek MA (2006) Methods for measuring denitrification: diverse approaches to a difficult problem. *Eco Apps* 16:2091–2122
- Haggard BE, Moore PA, DeLaune PB (2005) Phosphorus flux from bottom sediments in Lake Eucha. *Oklahoma J Env Qual* 34:724–728

- Harrison JA, Maranger RJ, Alexander RB, Giblin AE, Jacinthe PA, Mayorga E, Seitzinger SP, Sobota DJ, Wollheim WM (2009) The regional and global significance of nitrogen removal in lakes and reservoirs. *Biogeochemistry* 93:143–157
- Harrison MD, Groffman PM, Mayer PM, Kaushal SS (2012) Nitrate removal in two relict oxbow urban wetlands: a  $^{15}\text{N}$  mass-balance approach. *Biogeochemistry* 111:647–660
- Henderson KA, Murdock JN, Lizotte RE (2021) Water depth influences algal distribution and productivity in shallow agricultural lakes. *Ecohydrology* 14:e2319
- Hijmans RJ (2021) raster: geographic data analysis and modeling. R package version 3.4–13. <https://CRAN.R-project.org/package=raster>
- Hill AR, Kemp WA, Buttle JM, Goodyear D (1999) Nitrogen chemistry of subsurface storm runoff on forested Canadian Shield hillslopes. *Water Resour Res* 35:811–821. <https://doi.org/10.1029/1998WR900083>
- Inwood SE, Tank JL, Bernot MJ (2007) Factors controlling sediment denitrification in midwestern streams of varying land use. *Microb Ecol* 53:247–258. <https://doi.org/10.1007/s00248-006-9104-2>
- James WF (2010) Nitrogen retention in a floodplain backwater of the upper Mississippi River (USA). *Aquat Sci* 72:61–69
- Jeppesen E, Søndergaard M, Jensen JP, Havens KE, Anneville O, Carvahlo L, Coveney MF, Deneke R, Dokulil MT, Foy B, Gerdeaux D, Hampton SE, Hilt S, Kangur K, Kohler J, Lammens EH, Lauridsen TL, Manca M, Miracle MR, Moss B, Nöges P, Persson G, Phillips G, Portielje R, Romo S, Schelske CL, Straile D, Tatrai I, Willén E, Winder M (2005) Lake responses to reduced nutrient loading – an analysis of contemporary long-term data from 35 case studies. *Freshw Biol* 50:1747–1771. <https://doi.org/10.1111/j.1365-2427.2005.01415.x>
- Kana TM, Darkangelo C, Hunt MD, Oldham JB, Bennett GE, Cornwell JC (1994) Membrane inlet mass spectrometer for rapid high-precision determination of  $\text{N}_2$ ,  $\text{O}_2$ , and AR in environmental water samples. *Anal Chem* 66:4166–4170
- Katsev S, Tsandev I, L'Heureux I, Rancourt DG (2006) Factors controlling long-term phosphorus efflux from lake sediments: exploratory reactive-transport modeling. *Chem Geol* 234:127–147
- King KW, Williams MR, Johnson LT, Smith DR, LaBarge GA, Fausey NR (2017) Phosphorus availability in western Lake Erie Basin drainage waters: legacy evidence across spatial scale. *J Environ Qual* 46:466–469
- Knapp AN (2012) The sensitivity of marine  $\text{N}_2$  fixation to dissolved inorganic nitrogen. *Front Microbiol*. <https://doi.org/10.3389/fmicb.2012.00374>
- Knowles R (1982) Denitrification. *Microbiol Rev* 46:43–70
- Kraemer BM, Anneville O, Chandra S, Dix M, Kuusisto E, Livingstone DM, Rimmer A, Schladow SG, Silow E, Sitoki LM, Tamatamah R, Vadeboncoeur Y, McIntyre PB (2015) Morphometry and average temperature affect lake stratification responses to climate change. *Geophys Res Lett* 42:4981–4988
- Larson JH, James WF, Fitzpatrick FA, Frost PC, Evans MA, Reneau PC, Xenopoulos MA (2020) Phosphorus, nitrogen and dissolved organic carbon fluxes from sediments in freshwater rivermouths entering Green Bay (Lake Michigan; USA). *Biogeochemistry* 147:179–197
- Lehmann P, Hinz C, McGrath G, Tromp-van Meerveld HJ, McDonnell JJ (2007) Rainfall threshold for hillslope outflow: an emergent property of flow pathway connectivity. *Hydrol Earth Syst Sci* 11:1047–1063. <https://doi.org/10.5194/hess-11-1047-2007>
- Li H, Song C, Cao X, Zhou Y (2016) The phosphorus release pathways and their mechanisms driven by organic carbon and nitrogen in sediments of eutrophic shallow lakes. *Sci Total Environ* 572:280–288
- Li S, Christensen A, Twilley RR (2020) Benthic fluxes of dissolved oxygen and nutrients across hydrogeomorphic zones in a coastal deltaic floodplain within the Mississippi River delta plain. *Biogeochem* 149:115–140
- Li S, Twilley RR, Hou A (2021) Heterotrophic nitrogen fixation in response to nitrate loading and sediment organic matter in an emerging coastal deltaic floodplain within the Mississippi River Delta plain. *Limnol Oceanogr* 66:1961–1978. <https://doi.org/10.1002/lno.11737>
- Lizotte RE, Knight SS, Locke MA, Bingner RL (2014) Influence of integrated watershed-scale agricultural conservation practices on lake water quality. *J Soil Wat Conserv* 69:160–170
- Lizotte RE, Yasarer LMW, Locke MA, Bingner RL, Knight SS (2017) Lake nutrient responses to integrated conservation practices in an agricultural watershed. *J Environ Qual* 46:330–338
- Locke MA, Knight SS, Smith S, Cullum RF, Zablotowicz RM, Yuan Y, Bingner RL (2008) Environmental quality research in the Beasley Lake watershed, 1995 to 2007: succession from conventional to conservation practices. *J Soil Water Conserv* 63:430–442. <https://doi.org/10.2489/jswc.63.6.430>
- Locke MA (2004) Mississippi delta management systems evaluation area: overview of water quality issues on a watershed scale. In: Nett MT, Locke MA, Pennington DA, (Eds) *Water quality assessment in the Mississippi Delta: regional solutions, National scope*. ACS symposium series 877. American Chemical Society, Washington, DC
- Locke MA, Tyler DD, Gaston LA (2010) Soil and water conservation in the Mid-South United States: lessons learned and a look to the future. *Soil and Water Conservation Advances in the United States*. In: Zobeck TM, Schillinger WF (Eds). SSSA Special Publication 60. Madison, WI, USA
- Locke MA, Lizotte RE Jr, Yasarer LMW, Bingner RL, Moore MT (2020) Surface runoff in Beasley Lake watershed: Effect of land management practices in a Lower Mississippi River Basin watershed. *J Soil Water Conserv* 75:278–290
- Lorke A, Müller B, Maerki M, Wüest A (2003) Breathing sediments: the control of diffusive transport across the sediment–water interface by periodic boundary-layer turbulence. *Limnol Oceanogr* 48:2077–2085
- Matheson FE, Nguyen ML, Cooper AB, Burt TP, Bull DC (2002) Fate of  $^{15}\text{N}$ -nitrate in unplanted, planted and harvested riparian wetland soil microcosms. *Ecol Eng* 19:249–264

- McCarthy MJ, Gardner WS, Lavrentyev PJ, Moats KM, Jochem FJ, Klarer DM (2007) Effects of hydrological flow regime on sediment-water interface and water column nitrogen dynamics in a Great Lakes coastal wetland (Old Woman Creek, Lake Erie). *J Great Lakes Res* 33:219–231
- McCarthy MJ, Gardner WS, Lehmann MF, Guindon A, Bird DF (2016) Benthic nitrogen regeneration, fixation, and denitrification in a temperate, eutrophic lake: effects on the nitrogen budget and cyanobacteria blooms. *Limnol Oceanogr* 61:1406–1423
- Meals DW, Dressing SA, Davenport TE (2010) Lag time in water quality response to best management practices: a review. *J Environ Qual* 39:85–96
- Mengistu SG, Creed IF, Kulperger RJ, Quick CG (2013) Russian nesting dolls effect: using wavelet analysis to reveal non-stationary and nested stationary signals in water yield from catchments on a northern forested landscape. *Hydrol Process* 27:669–686. <https://doi.org/10.1002/hyp.9552>
- Miller-Way T, Twilley RR (1996) Theory and operation of continuous flow systems for the study of benthic-pelagic coupling. *Mar Ecol Prog Ser* 140:257–269
- Moriasi DN, Duriancik LF, Sadler EJ, Tsegaye T, Steiner JL, Locke MA, Strickland TC, Osmond DL (2020) Quantifying the impacts of the conservation effects assessment project watershed assessments: the first fifteen years. *J Soil Water Conserv* 75:57A–74A
- Mosier A, Kroeze C, Nevison C, Oenema O, Seitzinger S, van Cleemput O (1998) Closing the global N<sub>2</sub>O budget: nitrous oxide emissions through the agricultural nitrogen cycle. *Nutr Cycl Agroecosys* 52:225–248
- Newell SE, McCarthy MJ, Gardner WS, Fulweiler RW (2016a) Sediment nitrogen fixation: a call for re-evaluating coastal N budgets. *Est Coasts* 39:1626–1638
- Newell SE, Pritchard KR, Foster SQ, Fulweiler RW (2016b) Molecular evidence for sediment nitrogen fixation in a temperate New England estuary. *PeerJ* 4:e1615. <https://doi.org/10.7717/peerj.1615>
- Nielsen LP, Christensen PB, Revsbech NP, Sørensen J (1990) Denitrification and photosynthesis in stream sediment studied with microsensor and whole-core techniques. *Limnol Oceanogr* 35:1135–1144
- Nifong RL, Taylor JM, Moore MT (2019) Mulch-derived organic carbon stimulates high denitrification fluxes from agricultural ditch sediments. *J Environ Qual* 48:476–484. <https://doi.org/10.2134/jeq2018.09.0341>
- North RP, North RL, Livingstone DM, Koster O, Kipfer R (2014) Long-term changes in hypoxia and soluble reactive phosphorus in the hypolimnion of a large temperate lake: consequences of a climate regime shift. *Glob Chang Biol* 20:811–823
- Østergaard FA, Jensen HS (1992) Regeneration of inorganic phosphorus and nitrogen from decomposition of seston in a freshwater sediment. *Hydrobiologia* 228:71–81
- Paerl HW, Xu H, Hall NS, Rossignol KL, Joyner AR, Zhu G, Qin B (2015) Nutrient limitation dynamics examined on a multi-annual scale in Lake Taihu, China: implications for controlling eutrophication and harmful algal blooms. *J Freshw Ecol* 30:5–24
- Paerl HW, Havens KE, Xu H, Zhu G, McCarthy MJ, Newell SE, Scott JT, Hall NS, Otten TG, Qin B (2020) Mitigating eutrophication and toxic cyanobacterial blooms in large lakes: the evolution of a dual nutrient (N and P) reduction paradigm. *Hydrobiologia* 847:4359–4375
- Pinheiro J, Bates D, DebRoy S, Sarkar D, R Core Team (2020) nlme: linear and nonlinear mixed effects models. R package version 3.1–150. <https://CRAN.r-project.org/package=nlme>.
- Piña-Ochoa E, Álvarez-Cobelas M (2006) Denitrification in aquatic environments: a cross-system analysis. *Biogeochemistry* 81:111–130
- Poe AC, Piehler MF, Thompson SP, Paerl HW (2003) Denitrification in a constructed wetland receiving agricultural runoff. *Wetlands* 23:817–826
- R Core Team (2020) R: A language and environment for statistical computing. R Foundation for Statistical Computing, Vienna
- Reynolds CS (1998) What factors influence the species composition of phytoplankton in lakes of different trophic status? *Hydrobiologia* 369:11–26
- Reynolds CS (1999) Non-determinism to Probability, or N: P in the community ecology of phytoplankton. *Arch Hydrobiol* 146:23–35
- Royer TV, Tank JL, David MB (2004) Transport and fate of nitrate in headwater agricultural streams in Illinois. *J Environ Qual* 33:1296–1304. <https://doi.org/10.2134/jeq2004.1296>
- Royer TV, David MB (2005) Export of dissolved organic carbon from agricultural streams in Illinois. *USA Aquat Sci* 67:465–471. <https://doi.org/10.1007/s00027-005-0781-6>
- Sas H (1989) Lake restoration by reduction of nutrient loading. Expectation, experiences, extrapolation. Academia Verlag Richardz GmbH., St Augustin.
- Saunders DL, Kalf J (2001) Nitrogen retention in wetlands, lakes and rivers. *Hydrobiologia* 443:205–212
- Schilling KE, Wilke K, Pierce CL, Kult K, Kenny A (2019) Multipurpose oxbows as a nitrate export reduction practice in the agricultural Midwest. *Agric Environ Lett* 4:190035. <https://doi.org/10.2134/ael2019.09.0035>
- Scott JT, McCarthy MJ, Gardner WS, Doyle RD (2008) Denitrification, dissimilatory nitrate reduction to ammonium, and nitrogen fixation along a nitrate concentration gradient in a created freshwater wetland. *Biogeochemistry* 87:99–111
- Seitzinger SP (1988) Denitrification in freshwater and coastal marine ecosystems: ecological and geological significance. *Limnol Oceanogr* 33:702–724
- Seitzinger S, Harrison JA, Bohlke JK, Bouwman AF, Lowrance R, Peterson B, Tobias C, Van Drecht G (2006) Denitrification across landscapes and waterscapes: a synthesis. *Ecol App* 16:2064–2090
- Sen S, Haggard BE, Chaubey I, Brye KR, Costello TA, Matlock MD (2007) Sediment phosphorus release at beaver reservoir, Northwest Arkansas, USA, 2002–2003: a preliminary investigation. *Water Air Soil Pollut* 179:67–77. <https://doi.org/10.1007/s11270-006-9214-y>
- Sharpley A, Jarvie HP, Buda A, May L, Spears B, Kleinman P (2013) Phosphorus legacy: overcoming the effects of past management practices to mitigate future water quality impairment. *J Environ Qual* 42:1308–1326

- Simpson GL (2018) Modelling paleoecological time series using generalised additive models. *Front Ecol Evol* 6:149
- Small GE, Cotner JB, Findlay JC, Stark RA, Sterner RW (2014) Nitrogen transformations at the sediment–water interface across redox gradients in the Laurentian Great Lakes. *Hydrobiologia* 731:95–108. <https://doi.org/10.1007/s10750-013-1569-7>
- Song K, Burgin AJ (2017) Perpetual phosphorus cycling: eutrophication amplifies biological control on internal phosphorus loading in agricultural reservoirs. *Ecosystems* 20:1483–1493
- Song K, Adams CJ, Burgin AJ (2017) Relative importance of external and internal phosphorus loadings on affecting lake water quality in agricultural landscapes. *Ecol Engr* 108:482–488
- Stelzer RS, Bartsch LA, Richardson WB, Strauss EA (2011) The dark side of the hyporheic zone: depth profiles of nitrogen and its processing in stream sediments. *Freshw Biol* 56:2021–2033. <https://doi.org/10.1111/j.1365-2427.2011.02632.x>
- Tan E, Wenbin Z, Zheng Z, Yan X, Du M, Hsu T, Tian L, Midelburg JJ, Trull TW, Kao S (2020) Warming stimulates sediment denitrification at the expense of anaerobic ammonium oxidation. *Nat Clim Chang* 10:349–355. <https://doi.org/10.1038/s41558-020-0723-2>
- Taylor JM, Moore MT, Scott JT (2015) Contrasting nutrient mitigation and denitrification potential of agricultural drainage environments with different emergent aquatic macrophytes. *J Environ Qual* 44:1304–1314
- Taylor JM, Lizotte RE Jr, Testa S III (2019) Breakdown rates and associated nutrient cycling vary between novel crop-derived and natural riparian detritus in aquatic agroecosystems. *Hydrobiologia* 827:211–224
- Tiedje JM (1988) Ecology of denitrification and dissimilatory nitrate reduction to ammonium. In: Zehnder AJB (Ed). *Biology of anaerobic microorganisms*. New York, NY: John Wiley and Sons
- Trimmer M, Risgaard-Petersen N, Nicholls JC, Engström P (2006) Direct measurement of anaerobic ammonium oxidation (anammox) and denitrification in intact sediment cores. *Mar Ecol Prog Ser* 326:37–47
- USGS (2016) USGS historical topographic map explorer: Location: Indianola, Mississippi, United States. USGS, Reston, VA. <http://historicalmaps.arcgis.com/usgs/>. Accessed 29 July 2021
- Ullah S, Faulkner SP (2006) Denitrification potential of different land-use types in an agricultural watershed, lower Mississippi valley. *Ecol Engr* 28:131–140
- Van Meter KJ, Basu NB, Veenstra JJ, Burras CL (2016) The nitrogen legacy: emerging evidence of nitrogen accumulation in anthropogenic landscapes. *Environ Res Lett* 11:035014
- Vieillard AM, Fulweiler RW (2012) Impacts of long-term fertilization on salt marsh tidal creek benthic nutrient and N<sub>2</sub> gas fluxes. *Mar Ecol Prog Ser* 471:11–22
- Vymazal J (2007) Removal of nutrients in various types of constructed wetlands. *Sci Total Environ* 380:48–65
- Weiss RF (1970) The solubility of nitrogen, oxygen, and argon in water and seawater. *Deep-Sea Res* 17:721–735
- Welch EB, Cooke GD (2005) Internal phosphorus loading in shallow lakes: importance and control. *Lake and Reserv Manage* 11:273–281
- Wenk CB, Brees J, Zopfi J, Veronesi M, Bourbonnais A, Schubert CJ, Niemann H, Lehmann MF (2013) Anaerobic ammonium oxidation (anammox) bacteria and sulfide-dependent denitrifiers coexist in the water column of a meromictic south-alpine lake. *Limnol Oceanogr* 58:1–12
- Wood, S. N. 2017. *Generalized additive models, An introduction with R*. 2<sup>nd</sup> edition. Chapman and Hall/CRC. New York, New York.
- Wren DG, Taylor JM, Rigby JR, Locke MA, Yasarer LW (2019) Short term sediment accumulation rates reveal seasonal time lags between sediment delivery and deposition in an oxbow lake. *Agric Ecosyst Environ* 281:92–99
- Yao X, Zhang L, Zhang Y, Zhang B, Zhao Z, Zhang Y, Li M, Jiang X (2018) Nitrogen fixation occurring in sediments: contribution to the nitrogen budget of Lake Taihu. *China J Geophys Res Biogeosci* 123:2661–2674. <https://doi.org/10.1029/2018JG004466>
- Yasarer LMW, Bingner RL, Garbrecht JD, Locke MA, Lizotte RE Jr, Momm HG, Busteed PR (2017) Climate change impacts on runoff, sediment, and nutrient loads in an agricultural watershed in the Lower Mississippi River Basin. *Appl Eng Agric* 33:379–392
- Yoshii K, Melnik NG, Timoshkin OA, Bondarenko NA, Anoshko PN, Yoshioka T, Wada E (1999) Stable isotope analyses of the pelagic food web in Lake Baikal. *Limnol Oceanogr* 44:502–511
- Zhu G, Wang S, Wang S, Wang Y, Zhou L, Jiang B, Camp HJM, Risgaard-Petersen N, Schwark L, Peng Y, Hefting MM, Jetten MSM, Yin C (2013) Hotspots of anaerobic ammonium oxidation at land-freshwater interaces. *Nat Geosci* 6:103–107
- Zuur AF, Ieno EN, Walker N, Saveliev AA, Smith GM (2009) *Mixed effects models and extensions in ecology with R*. Springer, New York

**Publisher's Note** Springer Nature remains neutral with regard to jurisdictional claims in published maps and institutional affiliations.